Mechanics of Materials 58 (2013) 35–54

Contents lists available at SciVerse ScienceDirect

Mechanics of Materials

journal homepage: www.elsevier.com/locate/mechmat

The effect of a graded interphase on the mechanism of stress transfer in a fiber-reinforced composite

Yin Yao, Shaohua Chen *, Peijian Chen

LNM, Institute of Mechanics, Chinese Academy of Sciences, Beijing 100190, China

ARTICLE INFO

Article history:
Received 3 February 2012
Received in revised form 12 September 2012
Available online 1 December 2012

Keywords:
Fiber-reinforced composites
Graded interphase
Shear-lag model
Stress transfer
Shear failure

ABSTRACT

Based on an improved shear-lag model, the effect of an inhomogeneous interphase on the mechanism of stress transfer in fiber-reinforced composites is investigated. The inhomogeneity of the interphase is represented by the graded feature of the Young's modulus varying according to a power law or a linear one in the radius direction, while the Poisson's ratio and thermal expansion coefficient are assumed to be constants. Considering the effects of the inhomogeneous interphase as well as the Poisson's contraction and thermal residual stress, closed-form solutions to the axial fiber stress and interfacial shear stress are obtained analytically. Comparing the case with a power law to that with a linear one, we find that the fiber stress increases significantly in the former case, while it decreases slightly in the latter one with an increasing interphase thickness. With the same external tensile load and interphase thickness, it is found that the fiber in the power law case is subjected to a larger tensile stress than that in the linear variation one. However, the interfacial shear stress is not sensitive to the interphase thickness in both cases, except that near the two ends of fiber. Under the same external load, the maximum shear stress in the interphase is much smaller in the latter than that in the former. All the phenomena can be characterized by one parameter, i.e., the average Young's modulus of interphase, and denote that an interphase with a power variation law is more effective for stress transfer while the linearly graded one is more advantageous to avoid shear failure. The results should be helpful for engineers to properly design the interphase in novel composites, e.g. a carbon-fiber reinforced epoxy one.

1. Introduction

The mechanical properties of composites are affected by a number of factors, such as the volume fractions and constitutive behaviors of different constituents, some of which have been systematically reviewed in the recent papers (Fu et al., 2008; Lauke, 2006). Among the influencing factors, interphase, as one of the dominant elements, will show great significance on the composite performances (Yang and Pitchumani, 2004). During the process of manufacturing composites, physical and chemical interactions between reinforcements and matrix result in the formation of interphase encompassing the reinforcement/matrix interface (Drzal, 1986; Hughes, 1991; Theocaris, 1990; Williams et al., 1994). As an intermediate transition zone linking the reinforced fibers and matrix, the interphase plays a key role during the stress transfer between fibers and matrix (Hughes, 1991; Swain et al., 1990). Via proper design of an interphase zone in composites, the interfacial adhesion can be effectively improved, leading to a more efficient load transfer at interfaces. As a result, the overall stiffness and strength of composites can be enhanced since more external loads are sustained by the stiff reinforcements (Fu et al., 2008; Rjafiallah et al., 2010). Therefore, understanding and disclosing the micro-mechanism of stress transfer in fiber-reinforced composites with

* Corresponding author. Tel.: +86 10 82543960; fax: +86 10 82543977.
E-mail address: chenshaohua72@hotmail.com (S. Chen).

0167-6636/$ - see front matter
http://dx.doi.org/10.1016/j.mechmat.2012.11.008

interphase should be of great significance for the design of advanced composite materials.

Relevant experimental studies are relatively few due to the complexity of interphase composition, although the importance of the interphase has been fully acknowledged for a long time. The formation of an interphase depends directly on the chemical, mechanical and thermo-dynamical natures of the bonding process between fibers and matrix, which leads to spatially non-uniform properties of interphase in the thickness direction (Hughes, 1991; Gao and Mader, 2002; Liu et al., 2008; Naslain, 1998; Zhang et al., 2010). The size of an interphase region is rather small (at sub-microscopic scale) and experimental tests of the interfacial characteristics should be affected by many factors, such as the specimen geometries and fiber volume fractions (Atkins, 1975; Hughes, 1991; Liu et al., 2008; Zhang et al., 2010). An unequivocally experimental method to determine the realistic distributions of interphase properties is not yet available.

In contrast to a few experimental studies, a large number of theoretical and numerical investigations have been carried out in order to figure out how the interphase properties influence the overall mechanical behaviors of a fiber-reinforced composite. For simplicity, the interphase in many micromechanical models is assumed to be a homogeneous material (Christensen and Lo, 1979; Hashin, 1990; Hayes et al., 2001; Qiu and Weng, 1991; Rjafiallah et al., 2010; Tsai et al., 1990), or divided into many homogeneous sub-layers with different properties (Jiang et al., 2008; Mogilevskaya and Crouch, 2004; Wang et al., 2006). More realistic and accurate models regard the interphase as an inhomogeneous region with mechanical properties varying continuously in the thickness direction (Huang and Rokhlin, 1996; Jayaraman and Reifsnider, 1992, 1993; Kiritsi and Anifantis, 2001; Low et al., 1995; Lutz and Zimmerman, 2005; Romanowicz, 2010; Shen and Li, 2003), in which several empirical laws, such as power, linear and exponential ones, are used to describe the variations of the elastic modulus, Poisson's ratio or thermal expansion coefficient. Based on these models, the influences of an inhomogeneous interphase on the mechanical performances of composites, e.g. the thermal stress distribution and overall stiffness, can be qualitatively investigated.

Though a lot of attention has been paid to the effects of interphase properties on the stress transfer in a fiber-reinforced composite, most of them are numerical studies (Hayes et al., 2001; Kiritsi and Anifantis, 2001; Needleman et al., 2010; Wu et al., 1997). As for theoretical researches, the shear-lag model (Cox, 1952) is always chosen as a simple and effective approach, based on which a three-dimensional cylindrical or three-phase shear-lag model was often adopted (Afonso and Ranalli, 2005; Fu et al., 2000a,b; Monette et al., 1993; Tsai et al., 1990; Zhang and He, 2008). However, the interphase was also always modeled as a homogeneous material in these works. Few researchers used the shear-lag model to analyze the stress transfer in a fiber-reinforced composite with an inhomogeneous interphase.

In the present paper, an improved three-phase shear-lag model is established, in which an inhomogeneous interphase is taken into account. The inhomogeneity of the interphase is represented by a non-uniform Young's modulus, which varies according to a specially graded law, i.e., a power law and a linear one, while the Poisson's ratio and thermal expansion coefficient are assumed to be constants. An average interphase modulus, denoted as the integration of Young's modulus over the thickness divided by the interphase thickness, is introduced as a value to evaluate the effective stiffness of the inhomogeneous interphase. Then, the shear-lag governing equations for the two cases with differently graded laws are derived, in which the effects of Poisson's contraction and thermal residual stress are included too. Finally, the effects of interphase properties on the stress transfer in uni-directionally fiber-reinforced composites are explored. Comparisons are made for the two cases with different graded variations of interphase. The analytical solutions are also compared to the numerical ones in order to validate the constant assumptions of Poisson's ratio and thermal expansion coefficient in our model. The results in this paper should be helpful for optimal designs of an interfacial region in some novel composites with a thermosetting matrix and stiff fibers, e.g. carbon fiber-reinforced and carbon nanotube (CNT)-reinforced epoxy composites.

2. Basic model and general formulae

A three-phase concentrically cylindrical unit cell for a unidirectional fiber-reinforced composite is shown in Fig. 1, in which the cell is subjected to a uniform tensile load σ_0 at two ends and the lateral surfaces are traction free. The radius of the fiber cylinder is r_f and the length is L_f, surrounding which is a coaxially inhomogeneous interphase with the thickness t and radius r_i. Here $r_i = r_f + t$ as shown in Fig. 1. The radius of the matrix is r_m and the length is L_m. Thus, the volume fraction of fibers V_f in the fiber-reinforced composite can be expressed as

$$V_f = \frac{\pi r_f^2 L_f}{\pi r_m^2 L_m} = \frac{r_f^2 L_f}{r_m^2 L_m} \tag{1}$$

There are two interfaces in the three-phase model, i.e. the fiber/interphase interface and the interphase/matrix one, both of which are assumed to be perfect bonding. All the fiber, matrix and interphase are regarded as linear elastic and isotropic materials with E_f, ν_f, κ_f, E_m, ν_m, κ_m, E_i, ν_i, κ_i being their Young's moduli, Poisson's ratios and thermal expansion coefficients, respectively. The subscripts f, m and i represent the fiber, matrix and interphase. For simplicity, only the Young's modulus of the interphase is assumed to be spatially non-uniform in the radial direction, i.e., $E_i = E_i(r)$, while the Poisson's ratio and thermal expansion coefficient of the interphase are constants, as treated in Jayaraman and Reifsnider (1992) and Yang and Pitchumani (2004). In the following text, the constant assumptions of Poisson's ratio and thermal expansion coefficient will be proved to be reasonable. Then, an average modulus of the interphase can be defined as

$$\bar{E}_i = \frac{1}{r_i - r_f}\int_{r_f}^{r_i} E_i(r)dr = \frac{1}{t}\int_{r_f}^{r_i} E_i(r)dr, \tag{2}$$

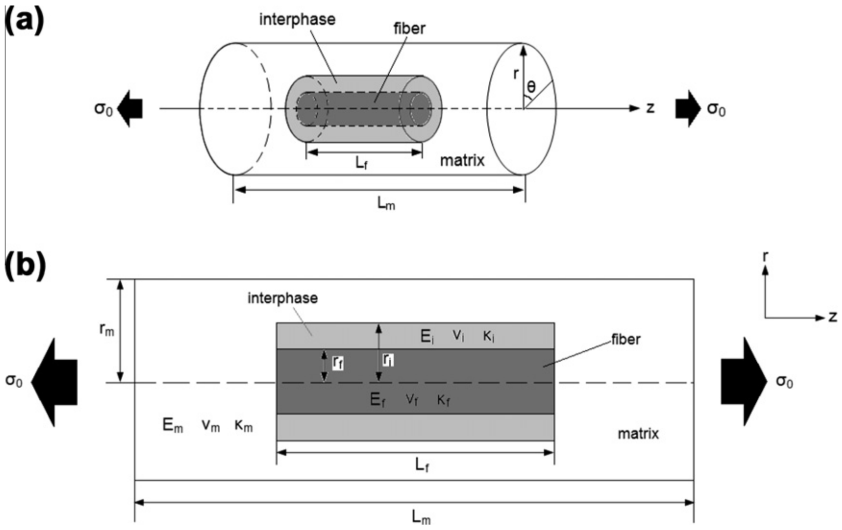

Fig. 1. (a) 3-D configuration of a three-phase cylindrical model of fiber-reinforced composites; (b) Schematic of the sizes of each phase in the model.

which can be used to evaluate the effective stiffness of the interphase (Jiang et al., 2008; Wang et al., 2006).

According to Fu et al. (2000a), Chai and Mai (2001) and Zhang and He (2008), the relations between the normal stresses in the fiber, interphase and matrix and the interfacial shear stresses at the two interfaces can be expressed as

$$\frac{d\sigma_f}{dz} = -\frac{2}{r_f}\tau_1; \quad \frac{d\sigma_i}{dz} = -\frac{2}{r_i^2 - r_f^2}(r_f\tau_1 - r_i\tau_2);$$
$$\frac{d\sigma_m}{dz} = \frac{2r_i}{r_m^2 - r_i^2}\tau_2 \tag{3}$$

which are the basic shear-lag equations for the three-phase composite system. σ_f, σ_i, σ_m are the normal stresses in the fiber, interphase and matrix, respectively, which depend on the coordinate z in the axial direction, i.e., $\sigma_f = \sigma_f(z)$, $\sigma_i = \sigma_i(z)$, $\sigma_m = \sigma_m(z)$. τ_1, τ_2, as functions of z, denote the interfacial shear stresses at the fiber/interphase and interphase/matrix interfaces, respectively. In addition, the equilibrium condition between the externally and internally axial stresses requires

$$\sigma_0 = \gamma_1\sigma_f(z) + \gamma_2\sigma_i(z) + \gamma_3\sigma_m(z)$$
$$\gamma_1 = \frac{r_f^2}{r_m^2}, \quad \gamma_2 = \frac{r_i^2 - r_f^2}{r_m^2}, \quad \gamma_3 = \frac{r_m^2 - r_i^2}{r_m^2} \tag{4}$$

As an improved shear-lag model, not only the axial stress but also the radial and hoop stresses in each phase of composites are considered. The stress–strain constitutive relations follow the general Hooke's law,

$$\varepsilon_\alpha^r = \frac{1}{E_\alpha}\left[\sigma_\alpha^r - \nu_\alpha(\sigma_\alpha^\theta + \sigma_\alpha)\right], \quad \varepsilon_\alpha^\theta = \frac{1}{E_\alpha}\left[\sigma_\alpha^\theta - \nu_\alpha(\sigma_\alpha^r + \sigma_\alpha)\right]$$
$$\varepsilon_\alpha^z = \frac{1}{E_\alpha}\left[\sigma_\alpha - \nu_\alpha(\sigma_\alpha^r + \sigma_\alpha^\theta)\right], \quad \varepsilon_\alpha^{rz} = \frac{2(1+\nu_\alpha)}{E_\alpha}\tau_\alpha^{rz} \quad (\alpha = f, i, m) \tag{5}$$

where $\sigma_\alpha^r, \sigma_\alpha^\theta, \sigma_\alpha, \tau_\alpha^{rz}$ are the radial, hoop, axial and shear stresses, and $\varepsilon_\alpha^r, \varepsilon_\alpha^\theta, \varepsilon_\alpha^z, \varepsilon_\alpha^{rz}$ are the corresponding strain components, respectively. The axial symmetric condition of the cylindrical model gives the following geometrical equations

$$\varepsilon_\alpha^r = \frac{\partial u_\alpha^r}{\partial r}, \quad \varepsilon_\alpha^\theta = \frac{u_\alpha^r}{r}, \quad \varepsilon_\alpha^z = \frac{\partial w_\alpha}{\partial z},$$
$$\varepsilon_\alpha^{rz} = \frac{\partial u_\alpha^r}{\partial z} + \frac{\partial w_\alpha}{\partial r} \quad (\alpha = f, i, m) \tag{6}$$

where $u_\alpha^r = u_\alpha^r(r,z)$ and $w_\alpha = w_\alpha(r,z)$ are the radial and axial displacements in different phases, the partial derivative of u_α^r with respect to z is ignored according to the treatment in Gao and Li (2005).

Eqs. (5) and (6) yield the interfacial shear stresses τ_1, τ_2 as (Chai and Mai, 2001; Zhang and He, 2008),

$$\tau_1 = \frac{1}{B_1 r_f}\left[\int_{r_f}^{r_i} \frac{E_i}{2(1+\nu_i)}\frac{\partial w_i(r,z)}{\partial r}dr + \frac{E_m}{2(1+\nu_m)}\frac{w_m(r_m,z) - w_i(r_i,z)}{B_3}B_2\right]$$
$$\tau_2 = \frac{E_m}{2(1+\nu_m)}\frac{w_m(r_m,z) - w_i(r_i,z)}{B_3 r_i} \tag{7}$$
$$B_1 = \frac{r_i^2}{r_i^2 - r_f^2}\ln\frac{r_i}{r_f} - \frac{1}{2}, \quad B_2 = \frac{r_f^2}{r_i^2 - r_f^2}\ln\frac{r_i}{r_f} - \frac{1}{2}, \quad B_3 = \frac{r_m^2}{r_m^2 - r_i^2}\ln\frac{r_m}{r_i} - \frac{1}{2}$$

Then, we have

$$\frac{d\tau_1}{dz} = \frac{1}{B_1 r_f}\left[\int_{r_f}^{r_i} \frac{E_i}{2(1+\nu_i)}\frac{\partial \varepsilon_i^z(r,z)}{\partial r}dr + \frac{E_m}{2(1+\nu_m)}\frac{\varepsilon_m^z(r_m,z) - \varepsilon_i^z(r_i,z)}{B_3}B_2\right] \tag{8}$$
$$\frac{d\tau_2}{dz} = \frac{E_m}{2(1+\nu_m)}\frac{\varepsilon_m^z(r_m,z) - \varepsilon_i^z(r_i,z)}{B_3 r_i} \tag{9}$$

In contrast to the study by Zhang and He (2008), the radial and hoop stresses in different phases are considered in the present paper. Moreover, the interphase in the present model is inhomogeneous, while a homogeneous interphase was considered in Zhang and He (2008). Two kinds of inhomogeneous characteristics of interphase, i.e., a power-graded variation law and a linearly graded one, will be analyzed as follows, respectively, based on the improved shear-lag model.

3. The case with a power-graded interphase

When the Young's modulus of the interphase follows a power variation law in the radial direction, i.e.,

$$E_i(r) = Pr^Q \tag{10}$$

The continuity conditions of the Young's modulus E_i at $r = r_f$ and $r = r_i$ yield

$$P = \frac{E_f}{r_f^Q} = \frac{E_m}{r_i^Q}, \quad Q = \frac{\ln E_m - \ln E_f}{\ln r_i - \ln r_f} \tag{11}$$

An average value of the interphase Young's modulus can be defined as

$$\overline{E}_i = \frac{1}{r_i - r_f}\int_{r_f}^{r_i} E_i(r)dr = \frac{E_f r_f}{(r_i - r_f)(Q+1)}\left[\left(\frac{r_i}{r_f}\right)^{Q+1} - 1\right] \tag{12}$$

The radial and hoop stresses in Eq. (5) consist of the ones induced by the Poisson's effect and the thermal residual stress (Chai and Mai, 2001; Liu et al., 1994),

$$\sigma_\alpha^r = \sigma_\alpha^{rp} + q_\alpha^r, \quad \sigma_\alpha^\theta = \sigma_\alpha^{\theta p} + q_\alpha^\theta \quad (\alpha = f, i, m) \tag{13}$$

where σ_α^{rp} and $\sigma_\alpha^{\theta p}$ denote the radial and hoop stresses arising from Poisson's contraction, q_α^r and q_α^θ are the corresponding components of thermal residual stresses developed during the initial fabrication of composites (Gao et al., 1988), as shown in Fig. 2. Next, the formulations of $\sigma_\alpha^{rp}, \sigma_\alpha^{\theta p}$ and $q_\alpha^r, q_\alpha^\theta$ will be found separately.

3.1. The radial and hoop stresses due to Poisson's contraction

Under an external load σ_0, the axial stresses in the fiber, interphase and matrix are σ_f, σ_i, σ_m. The radial and hoop stresses $\sigma_f^{rp}, \sigma_f^{\theta p}, \sigma_m^{rp}, \sigma_m^{\theta p}$ in the homogeneous fiber and matrix can be easily obtained (Gao et al., 1988; Whitney and Riley, 1966),

$$\sigma_f^{rp} = \sigma_f^{\theta p} = A, \quad \sigma_m^{rp} = \frac{F}{r^2} + H, \quad \sigma_m^{\theta p} = -\frac{F}{r^2} + H \tag{14}$$

where the unknown parameters A, F, H are independent of r.

Using Eqs. (5) and (6) leads to the radial and hoop stresses in the inhomogeneous interphase,

$$\begin{aligned}
\sigma_i^{rp} &= \frac{E_i}{I_i}\left[(1-v_i^2)\frac{du_i^r}{dr} + v_i(1+v_i)\left(\frac{u_i^r}{r} + \varepsilon_i^z\right)\right] \\
\sigma_i^{\theta p} &= \frac{E_i}{I_i}\left[(1-v_i^2)\frac{u_i^r}{r} + v_i(1+v_i)\left(\frac{du_i^r}{dr} + \varepsilon_i^z\right)\right] \\
\varepsilon_i^z &= \frac{1}{1-v_i^2}\left[\frac{I_i}{E_i}\sigma_i - v_i(1+v_i)\left(\frac{du_i^r}{dr} + \frac{u_i^r}{r}\right)\right]
\end{aligned} \tag{15}$$

where $I_i = (1 + v_i)^2(1 - 2v_i)$.

The equilibrium equation for the interphase is

$$\frac{d\sigma_i^{rp}}{dr} + \frac{\sigma_i^{rp} - \sigma_i^{\theta p}}{r} = 0 \tag{16}$$

Substituting Eq. (15) into (16) yields

$$\begin{aligned}
&\frac{d^2u_i^r}{dr^2} + \left(\frac{dE_i}{dr}\frac{1}{E_i} + \frac{1}{r}\right)\frac{du_i^r}{dr} + \left(\frac{1}{r}\frac{dE_i}{dr}\frac{v_i}{E_i(1-v_i)} - \frac{1}{r^2}\right)u_i^r \\
&\quad + \frac{dE_i}{dr}\frac{v_i}{E_i(1-v_i)}\varepsilon_i^z + \frac{v_i}{1-v_i}\frac{\partial\varepsilon_i^z}{\partial r} = 0
\end{aligned} \tag{17}$$

Substituting ε_i^z in Eqs. (15) and (10) into Eq. (17), we get

$$\frac{d^2u_i^r}{dr^2} + \left(\frac{Q+1}{r}\right)\frac{du_i^r}{dr} + \left(\frac{Qv_i - 1}{r^2}\right)u_i^r = 0 \tag{18}$$

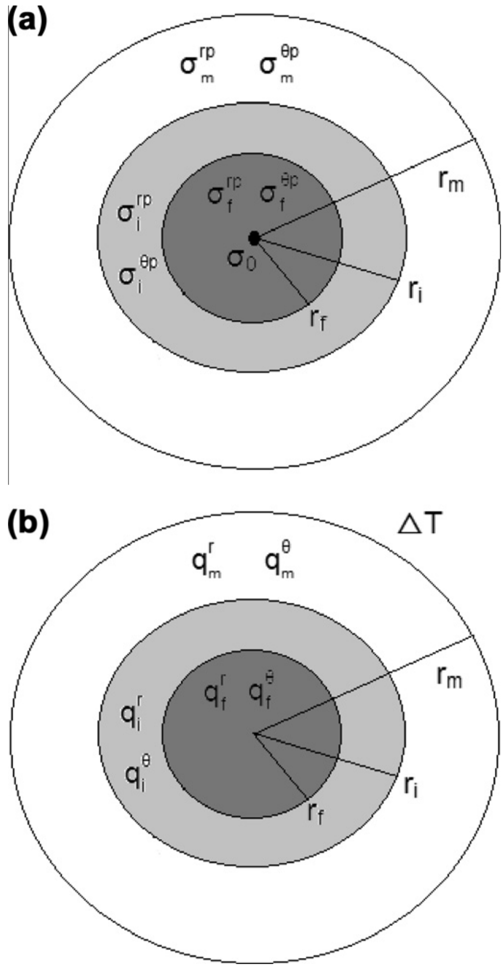

Fig. 2. (a) Radial and hoop stresses induced by the Poisson's effect when the cell is subjected to a mechanical load σ_0 orthogonal to the $r - \theta$ plane; (b) Thermal residual stresses arising from temperature changes during the initial fabrication of composites.

Solving Eq. (18) yields

$$u_i^r = Br^{m_1} + Cr^{m_2}, \quad m_{1,2} = \frac{1}{2}\left[-Q \pm \sqrt{Q^2 - 4(Qv_i - 1)}\right] \tag{19}$$

where B, C are two unknown parameters to be determined by the boundary conditions. Then, the radial and hoop strains in the interphase are obtained

$$\begin{aligned}
\varepsilon_i^r &= \frac{du_i^r}{dr} = m_1Br^{m_1-1} + m_2Cr^{m_2-1}, \\
\varepsilon_i^\theta &= \frac{u_i^r}{r} = Br^{m_1-1} + Cr^{m_2-1}
\end{aligned} \tag{20}$$

Combining Eqs. (10), (15) and (20) leads to,

$$\begin{aligned}
\sigma_i^{rp} &= \frac{P}{I_i}\left[A_1Br^{-(m_2+1)} + A_2Cr^{-(m_1+1)}\right] + \frac{v_i}{1-v_i}\sigma_i \\
\sigma_i^{\theta p} &= \frac{P}{I_i}\left[A_3Br^{-(m_2+1)} + A_4Cr^{-(m_1+1)}\right] + \frac{v_i}{1-v_i}\sigma_i \\
\sigma_i^{rp} + \sigma_i^{\theta p} &= \frac{P}{I_i}\left[A_5Br^{-(m_2+1)} + A_6Cr^{-(m_1+1)}\right] + \frac{2v_i}{1-v_i}\sigma_i
\end{aligned} \tag{21}$$

where

$$A_1=(m_1+\nu_i)\frac{(1+\nu_i)(1-2\nu_i)}{1-\nu_i},\quad A_2=(m_2+\nu_i)\frac{(1+\nu_i)(1-2\nu_i)}{1-\nu_i},$$
$$A_3=(m_1\nu_i+1)\frac{(1+\nu_i)(1-2\nu_i)}{1-\nu_i},\quad A_4=(m_2\nu_i+1)\frac{(1+\nu_i)(1-2\nu_i)}{1-\nu_i},$$
$$A_5=A_1+A_3,\quad A_6=A_2+A_4 \tag{22}$$

Five unknown parameters A, B, C, F, H are included in Eqs. (14) and (21). Consider the boundary conditions (Song et al., 1996; Zhang et al., 2010),

$$r=r_f:\quad \sigma_f^{rp}=\sigma_i^{rp},\quad u_f^r=u_i^r \tag{23}$$
$$r=r_i:\quad \sigma_i^{rp}=\sigma_m^{rp},\quad u_i^r=u_m^r \tag{24}$$
$$r=r_m:\quad \sigma_m^{rp}=0 \tag{25}$$

We have

$$\begin{cases} A=\frac{1}{H_4}(H_1\sigma_f+H_2\sigma_i+H_3\sigma_m)\\ B=\dfrac{\left(\frac{r_i}{r_f}\right)^{m_2-1}F_4(S_1\sigma_i-\nu_f\sigma_f)-\frac{E_f}{E_m}F_2(S_2\sigma_i-\nu_m\sigma_m)}{E_fr_f^{m_1-1}\left(\frac{r_i}{r_f}\right)^{m_2-1}F_1F_4-E_fr_i^{m_1-1}F_2F_3}\\ C=\dfrac{\left(\frac{r_i}{r_f}\right)^{m_1-1}F_3(S_1\sigma_i-\nu_f\sigma_f)-\frac{E_f}{E_m}F_1(S_2\sigma_i-\nu_m\sigma_m)}{E_fr_f^{m_2-1}\left(\frac{r_i}{r_f}\right)^{m_1-1}F_2F_3-E_fr_i^{m_2-1}F_1F_4}\\ F=-r_m^2H\\ H=-\frac{r_i^2}{r_m^2-r_i^2}\frac{1}{H_8}(H_5\sigma_f+H_6\sigma_i+H_7\sigma_m)\end{cases} \tag{26}$$

Then, the radial and hoop stresses in different phases can be obtained, which are functions of the axial stresses σ_f, σ_i, σ_m. In addition, we have

$$\begin{aligned}\left(\sigma_i^{rp}+\sigma_i^{\theta p}\right)_{r=r_f}&=\frac{1}{H_4}(H_9\sigma_f+H_{10}\sigma_i+H_{11}\sigma_m)\\ \left(\sigma_i^{rp}+\sigma_i^{\theta p}\right)_{r=r_i}&=\frac{1}{H_8}(H_{12}\sigma_f+H_{13}\sigma_i+H_{14}\sigma_m)\end{aligned} \tag{27}$$

Parameters $F_1\sim F_4$, $H_1\sim H_{14}$, S_1 and S_2 are given in Appendix A.

3.2. Thermal residual stress

In the initial fabrication process, shrinkage or expansion occurs in the composite constituents due to the temperature change, which gives rise to thermal stresses in different phases because of their different thermal expansion coefficients. According to Jayaraman and Reifsnider (1992, 1993), the solutions of the radial displacement induced by thermal effects can be given directly. In the homogeneous fiber and matrix, we have

$$\bar{u}_f^r=\bar{A},\quad \bar{u}_m^r=\bar{H}r+\frac{\bar{F}}{r} \tag{28}$$

which leads to the stress components $q_f^r, q_f^\theta, q_m^r, q_m^\theta$ with the same forms as those in Eq. (14). Here, the notation "-" on a variable denotes the relevance to the thermal effects (the same hereinafter).

The radial displacement in the interphase is

$$\begin{aligned}\bar{u}_i^r(r)&=\bar{B}r^{\bar{m}_1}+\bar{C}r^{\bar{m}_2}-\nu_i\bar{D}r,\\ \bar{m}_{1,2}&=\frac{1}{2}\left[-Q\pm\sqrt{Q^2-4\left(\frac{Q\nu_i}{1-\nu_i}-1\right)}\right]\end{aligned} \tag{29}$$

where $\bar{D}$ equals to the axial strain induced by the thermal effects and can be determined by the vanishing axial stress condition. Then, the radial and hoop stresses in the interphase can be obtained,

$$\begin{aligned}q_i^r&=\frac{P}{I_i}\left[\bar{A}_1\bar{B}r^{-(\bar{m}_2+1)}+\bar{A}_2\bar{C}r^{-(\bar{m}_1+1)}\right]\\ q_i^\theta&=\frac{P}{I_i}\left[\bar{A}_3\bar{B}r^{-(\bar{m}_2+1)}+\bar{A}_4\bar{C}r^{-(\bar{m}_1+1)}\right]\\ q_i^r+q_i^\theta&=\frac{P}{I_i}\left[\bar{A}_5\bar{B}r^{-(\bar{m}_2+1)}+\bar{A}_6\bar{C}r^{-(\bar{m}_1+1)}\right]\end{aligned} \tag{30}$$

in which we have

$$\bar{A}_1=\bar{m}_1(1-\nu_i^2)+\nu_i(1+\nu_i),\bar{A}_2=\bar{m}_2(1-\nu_i^2)+\nu_i(1+\nu_i),$$
$$\bar{A}_3=(1-\nu_i^2)+\bar{m}_1\nu_i(1+\nu_i),\bar{A}_4=(1-\nu_i^2)+\bar{m}_2\nu_i(1+\nu_i),$$
$$\bar{A}_5=\bar{A}_1+\bar{A}_3,\quad \bar{A}_6=\bar{A}_2+\bar{A}_4 \tag{31}$$

In order to determine the parameters $\bar{A},\bar{B},\bar{C},\bar{D},\bar{F},\bar{H}$, six boundary conditions are required (Jayaraman and Reifsnider, 1992; Zhang et al., 2010),

$$r=r_f:\quad q_f^r=q_i^r,\quad \bar{u}_f^r+\alpha_f\Delta T=\bar{u}_i^r+\alpha_i\Delta T \tag{32}$$
$$r=r_i:\quad q_i^r=q_m^r,\quad \bar{u}_i^r+\alpha_i\Delta T=\bar{u}_m^r+\alpha_m\Delta T \tag{33}$$
$$r=r_m:\quad q_m^r=0 \tag{34}$$
$$\int_0^{r_f}\bar{\sigma}_f^z rdr+\int_{r_f}^{r_i}\bar{\sigma}_i^z rdr+\int_{r_i}^{r_m}\bar{\sigma}_m^z rdr=0,\quad \text{(zero-axial stress condition)} \tag{35}$$

Using the above boundary conditions yields

$$\begin{cases}\bar{A}=K_1\bar{D}+K_2q_1+K_3q_2\\ \bar{B}=\dfrac{(r_i/r_f)^{m_2-1}\bar{F}_4[q_1\Delta T+(\nu_i-\nu_f)\bar{D}]-\bar{F}_2[q_2\Delta T+(\nu_i-\nu_m)\bar{D}]}{r_f^{m_1-1}(r_i/r_f)^{m_2-1}\bar{F}_1\bar{F}_4-r_i^{m_1-1}\bar{F}_2\bar{F}_3}\\ \bar{C}=\dfrac{(r_i/r_f)^{m_1-1}\bar{F}_3[q_1\Delta T+(\nu_i-\nu_f)\bar{D}]-\bar{F}_1[q_2\Delta T+(\nu_i-\nu_m)\bar{D}]}{r_f^{m_2-1}(r_i/r_f)^{m_1-1}\bar{F}_2\bar{F}_3-r_i^{m_2-1}\bar{F}_1\bar{F}_4}\\ \bar{F}=K_4\bar{D}+K_5q_1+K_6q_2\\ \bar{H}=\frac{r_m^2}{1-2\nu_m}[(K_4+\nu_m)\bar{D}+K_5q_1+K_6q_2]\\ \bar{D}=-\frac{1}{K_7}(K_8q_1+K_9q_2)\end{cases} \tag{36}$$

where $q_1=(\alpha_f-\alpha_i)\Delta T$, $q_2=(\alpha_m-\alpha_i)\Delta\ T$. In addition, the general forms of $q_\alpha^r+q_\alpha^\theta(\alpha=f,i,m)$ in different phases are found,

$$
\begin{aligned}
Q_1 &= q_f^r + q_f^\theta = \frac{2E_f}{I_f}(1+\nu_f)\left\{\left[K_2 - \frac{K_8}{K_7}(K_1+\nu_f)\right]q_1 + \left[K_3 - \frac{K_9}{K_7}(K_1+\nu_f)\right]q_2\right\}\\
Q_2 &= q_m^r + q_m^\theta = \frac{2E_m}{I_m}(1+\nu_m)\left\{\left[K_5 - \frac{K_8}{K_7}(K_4+\nu_m)\right]q_1 + \left[K_6 - \frac{K_9}{K_7}(K_4+\nu_m)\right]q_2\right\}\\
Q_3 &= (q_i^r + q_i^\theta)_{r=r_f} = \left(K_{11} - K_{10}\frac{K_8}{K_7}\right)q_1 + \left(K_{12} - K_{10}\frac{K_9}{K_7}\right)q_2\\
Q_4 &= (q_i^r + q_i^\theta)_{r=r_i} = \left(K_{14} - K_{13}\frac{K_8}{K_7}\right)q_1 + \left(K_{15} - K_{13}\frac{K_9}{K_7}\right)q_2
\end{aligned}
\tag{37}
$$

Parameters $K_1 \sim K_{15}, \overline{F}_1 \sim \overline{F}_4$ are given in Appendix A.

3.3. Stresses in the improved shear-lag model

In Sections 3.1 and 3.2, we have obtained the radial and hoop stresses induced by the Poisson's and thermal effects for a fiber-reinforced composite with an inhomogeneous interphase. With the help of the above results, the axial stresses in fiber, interphase and matrix can be found. Considering equations (5), (10), (13), (21) and (30), we obtain the axial strain ε_i^z in the interphase

$$
\begin{aligned}
\varepsilon_i^z(r,z) &= \frac{1}{E_i}\left[\sigma_i - \nu_i(\sigma_i^r + \sigma_i^\theta)\right]\\
&= \left(1 - \frac{2\nu_i^2}{1-\nu_i}\right)\frac{\sigma_i}{Pr^Q} - \frac{\nu_i}{I_i r^Q}\left[A_5 B r^{-(m_2+1)} + A_6 C r^{-(m_1+1)}\right.\\
&\quad \left. + \overline{A}_5\overline{B} r^{-(\overline{m}_2+1)} + \overline{A}_6\overline{C} r^{-(\overline{m}_1+1)}\right]
\end{aligned}
\tag{38}
$$

The derivative of ε_i^z with respect to r is

$$
\begin{aligned}
\frac{\partial \varepsilon_i^z}{\partial r} &= -\left(1 - \frac{2\nu_i^2}{1-\nu_i}\right)\frac{\sigma_i Q}{Pr^{Q+1}}\\
&\quad - \frac{\nu_i}{I_i}\left[A_5 B(m_1-1)r^{m_1-2} + A_6 C(m_2-1)r^{m_2-2}\right.\\
&\quad \left. + \overline{A}_5\overline{B}(\overline{m}_1-1)r^{\overline{m}_1-2} + \overline{A}_6\overline{C}(\overline{m}_2-1)r^{\overline{m}_2-2}\right]
\end{aligned}
\tag{39}
$$

Then, the integral in Eq. (8) can be written as,

$$
\begin{aligned}
\int_{r_f}^{r_i} \frac{E_i}{2(1+\nu_i)}\frac{\partial \varepsilon_i^z(r,z)}{\partial r}dr &= -\left(1 - \frac{2\nu_i^2}{1-\nu_i}\right)\frac{\ln(r_i/r_f)}{2(1+\nu_i)}Q\sigma_i\\
&\quad + \frac{\nu_i}{2I_i(1+\nu_i)}\left[C_1\sigma_f + C_2\sigma_i + C_3\sigma_m + Q_5\right]
\end{aligned}
\tag{40}
$$

where

$$
Q_5 = \left(C_5 - C_4\frac{K_8}{K_7}\right)q_1 + \left(C_6 - C_4\frac{K_9}{K_7}\right)q_2 \tag{41}
$$

Another term in Eqs. (8) and (9) can also be derived

$$
\begin{aligned}
\varepsilon_m^z(r_m,z) - \varepsilon_i^z(r_i,z) &= \frac{\nu_i}{E_i}Q_4 - \frac{\nu_m}{E_m}Q_2\\
&\quad + \left[\frac{2\nu_m r_i^2}{E_m(r_m^2 - r_i^2)}\frac{H_5}{H_8} + \frac{\nu_i}{E_i}\frac{H_{12}}{H_8}\right]\sigma_f\\
&\quad + \left[\frac{2\nu_m r_i^2}{E_m(r_m^2 - r_i^2)}\frac{H_6}{H_8} - \frac{1}{E_i} + \frac{\nu_i}{E_i}\frac{H_{13}}{H_8}\right]\sigma_i\\
&\quad + \left[\frac{1}{E_m}\left(1 + \frac{2\nu_m r_i^2}{r_m^2 - r_i^2}\frac{H_7}{H_8}\right) + \frac{\nu_i}{E_i}\frac{H_{14}}{H_8}\right]\sigma_m
\end{aligned}
\tag{42}
$$

where Q_2 and Q_4 are given in Eq. (37). Combining Eqs. (8), (9), (40) and (42) results in

$$
\begin{aligned}
\frac{d\tau_1}{dz} &= \frac{1}{B_1 r_f}(C_7\sigma_f + C_8\sigma_i + C_9\sigma_m + Q_6)\\
\frac{d\tau_2}{dz} &= \frac{1}{2(1+\nu_m)B_3 r_i}(C_{10}\sigma_f + C_{11}\sigma_i + C_{12}\sigma_m + Q_7)\\
Q_6 &= -\frac{B_2}{2(1+\nu_m)B_3}\left(\nu_m Q_2 - \frac{E_m}{E_i}\nu_i Q_4\right) + \frac{\nu_i}{2I_i(1+\nu_i)}Q_5\\
Q_7 &= -\nu_m Q_2 + \frac{E_m}{E_i}\nu_i Q_4
\end{aligned}
\tag{43}
$$

The relevant parameters $C_1 \sim C_{12}$ are given in Appendix A.

Substituting Eq. (43) into (3) leads to

$$
\begin{aligned}
\frac{d^2\sigma_f}{dz^2} &= -\frac{2}{r_f}\frac{d\tau_1}{dz} = -\frac{2}{B_1 r_f^2}(C_7\sigma_f + C_8\sigma_i + C_9\sigma_m + Q_6)\\
\frac{d^2\sigma_i}{dz^2} &= \frac{2}{r_i^2 - r_f^2}\left(r_f\frac{d\tau_1}{dz} - r_i\frac{d\tau_2}{dz}\right) = \frac{2}{r_i^2 - r_f^2}\left[\frac{1}{B_1}(C_7\sigma_f + C_8\sigma_i + C_9\sigma_m + Q_6)\right.\\
&\quad \left. - \frac{1}{2(1+\nu_m)B_3}(C_{10}\sigma_f + C_{11}\sigma_i + C_{12}\sigma_m + Q_7)\right]\\
\frac{d^2\sigma_m}{dz^2} &= \frac{2r_i}{r_m^2 - r_i^2}\frac{d\tau_2}{dz} = \frac{1}{(1+\nu_m)(r_m^2 - r_i^2)B_3}(C_{10}\sigma_f + C_{11}\sigma_i + C_{12}\sigma_m + Q_7)
\end{aligned}
\tag{44}
$$

In addition, Eq. (4) yields,

$$
\sigma_m = \frac{1}{\gamma_3}(\sigma_0 - \gamma_1\sigma_f - \gamma_2\sigma_i) \tag{45}
$$

Then, the axial stress σ_i in the interphase can be obtained by substituting Eq. (45) into the first equation of (44)

$$
\sigma_i = -\frac{\frac{B_1 r_f^2}{2}\frac{d^2\sigma_f}{dz^2} + \left(C_7 - \frac{\gamma_1}{\gamma_3}C_9\right)\sigma_f - \left(Q_6 + \frac{C_9}{\gamma_3}\sigma_0\right)}{C_8 - \frac{\gamma_2}{\gamma_3}C_9} \tag{46}
$$

Further substituting Eq. (46) into the second equation of (44) yields a fourth-order ordinary differential equation about σ_f,

$$
\frac{d^4\sigma_f}{dz^4} + S_{11}\frac{d^2\sigma_f}{dz^2} + S_{22}\sigma_f + S_{33} = 0 \tag{47}
$$

in which

$$
\begin{aligned}
S_{11} &= \frac{2}{B_1 r_f^2}\left(C_7 - \frac{\gamma_1}{\gamma_3}C_9\right) - \frac{2}{B_1\left(r_i^2 - r_f^2\right)}\left[\left(C_8 - \frac{\gamma_2}{\gamma_3}C_9\right) - \frac{1}{2(1+\nu_m)B_3}\left(C_{11} - \frac{\gamma_2}{\gamma_3}C_{12}\right)\right]\\
S_{22} &= \frac{2}{B_1 r_f^2\left(r_i^2 - r_f^2\right)}\frac{1}{(1+\nu_m)B_3}\left[\left(C_{11} - \frac{\gamma_2}{\gamma_3}C_{12}\right)\left(C_7 - \frac{\gamma_1}{\gamma_3}C_9\right) - \left(C_8 - \frac{\gamma_2}{\gamma_3}C_9\right)\left(C_{10} - \frac{\gamma_1}{\gamma_3}C_{12}\right)\right]\\
S_{33} &= \frac{2}{B_1 r_f^2\left(r_i^2 - r_f^2\right)}\frac{1}{(1+\nu_m)B_3}\left[\left(C_{11} - \frac{\gamma_2}{\gamma_3}C_{12}\right)\left(Q_6 + \frac{C_9}{\gamma_3}\sigma_0\right) - \left(C_8 - \frac{\gamma_2}{\gamma_3}C_9\right)\left(Q_7 + \frac{C_{12}}{\gamma_3}\sigma_0\right)\right]
\end{aligned}
\tag{48}
$$

Using the non-dimensional parameters $r^* = r/r_f, z^* = z/L_f$, $r_i^* = r_i/r_f, r_m^* = r_m/r_f$ and $t^* = t/r_f = r_i^* - 1$, Eq. (47) can be rewritten as

$$
\frac{d^4\sigma_f}{dz^{*4}} + 4\rho^2 S_{11}^*\frac{d^2\sigma_f}{dz^{*2}} + 16\rho^4 S_{22}^*\sigma_f + 16\rho^4 S_{33}^* = 0 \tag{49}
$$

where $\rho = L_f/2r_f$ denotes the aspect ratio of the cylindrical fiber and the dimensionless parameters $S_{11}^*, S_{22}^*, S_{33}^*$ are

$$
\begin{aligned}
S_{11}^* &= \frac{2}{B_1}\left(C_7 - \frac{\gamma_1}{\gamma_3}C_9\right) - \frac{2}{B_1\left[(1+t^*)^2 - 1\right]}\left[\left(C_8 - \frac{\gamma_2}{\gamma_3}C_9\right) - \frac{1}{2(1+\nu_m)B_3}\left(C_{11} - \frac{\gamma_2}{\gamma_3}C_{12}\right)\right]\\
S_{22}^* &= \frac{2}{B_1 B_3(1+\nu_m)[(1+t^*)^2 - 1]}\left[\left(C_{11} - \frac{\gamma_2}{\gamma_3}C_{12}\right)\left(C_7 - \frac{\gamma_1}{\gamma_3}C_9\right) - \left(C_8 - \frac{\gamma_2}{\gamma_3}C_9\right)\left(C_{10} - \frac{\gamma_1}{\gamma_3}C_{12}\right)\right]\\
S_{33}^* &= \frac{2}{B_1 B_3(1+\nu_m)[(1+t^*)^2 - 1]}\left[\left(C_{11} - \frac{\gamma_2}{\gamma_3}C_{12}\right)\left(Q_6 + \frac{C_9}{\gamma_3}\sigma_0\right) - \left(C_8 - \frac{\gamma_2}{\gamma_3}C_9\right)\left(Q_7 + \frac{C_{12}}{\gamma_3}\sigma_0\right)\right]
\end{aligned}
\tag{50}
$$

According to Afonso and Ranalli (2005) and Fu et al. (2000a,b), the general solution to Eq. (49) can be obtained as

$$\sigma_f(z^*) = -\frac{S_{33}^*}{S_{22}^*} + W_3\cosh(k_1 z^*) + W_4\cosh(k_1 z^*)$$
$$k_1 = 2\rho\sqrt{\frac{-S_{11}^* - \sqrt{S_{11}^{*2} - 4S_{22}^*}}{2}} \quad (0 \leqslant z^* \leqslant 1) \tag{51}$$

Due to the assumption of perfectly bonded interfaces in the present model, we have $\sigma_f(0) = \sigma_0$ and $\sigma_f(1) = \sigma_0$, which yield

$$W_3 = \sigma_0 + \frac{S_{33}^*}{S_{22}^*}$$
$$W_4 = \frac{\left(\sigma_0 + \frac{S_{33}^*}{S_{22}^*}\right)[1 - \cosh(k_1)]}{\sinh(k_1)} \tag{52}$$

Then, the normalized closed-form solution of fiber's axial stress is

$$\sigma_f^* = \frac{\sigma_f(z^*)}{\sigma_0} = \frac{-\frac{S_{33}^*}{S_{22}^*} + \left(\sigma_0 + \frac{S_{33}^*}{S_{22}^*}\right)\frac{\sinh[k_1(1-z^*)]}{\sinh(k_1)} + \left(\sigma_0 + \frac{S_{33}^*}{S_{22}^*}\right)\frac{\sinh(k_1 z^*)}{\sinh(k_1)}}{\sigma_0} \tag{53}$$

4. The case with a linearly graded interphase

When the Young's modulus of the interphase follows a linear variation law in the radial direction, i.e.,

$$E_i(r) = a + br \tag{54}$$

The continuity conditions of the Young's modulus E_i at $r = r_f$ and $r = r_i$ yield

$$a = \frac{r_i}{r_i - r_f}E_f - \frac{r_f}{r_i - r_f}E_m, \quad b = -\frac{E_f - E_m}{r_i - r_f} \tag{55}$$

The average interphase modulus is

$$\bar{E}_i = \frac{E_f + E_m}{2} \tag{56}$$

In contrast to the average interphase modulus in Eq. (12), $\bar{E}_i$ is a constant in this case, which is independent of the interphase size.

The similar method to that in Section 3 can be used to find the radial and hoop stresses induced by Poisson's contraction and thermal residual stress, respectively.

4.1. The radial and hoop stresses due to Poisson's contraction

In the homogeneous fiber and matrix, the radial and hoop stresses have the same forms as those in Eq. (14), and the equilibrium equation in the interphase can be written as

$$\frac{d^2u_i^r}{dr^2} + \left(\frac{b}{a+br} + \frac{1}{r}\right)\frac{du_i^r}{dr} + \left(\frac{b\nu_i}{r(a+br)} - \frac{1}{r^2}\right)u_i^r = 0 \tag{57}$$

Let $\frac{b}{a+br} + \frac{1}{r} = p(r)$ and $\frac{b\nu_i}{r(a+br)} - \frac{1}{r^2} = q(r)$. The general solution to Eq. (57) can be found using the series solution method (Johnson and Johnson, 1965). One can see that two singular points exist in $p(r)$ and $q(r)$, i.e. $r = 0$ and $r = -a/b$. However, both of them lie outside the interphase domain. Eq. (57) can be solved as (Jayaraman and Reifsnider, 1992, 1993)

$$u_i^r(r) = \sum_{n=0}^{\infty} R_n(r - r_0)^n, \quad r_0 = \frac{r_i + r_f}{2} \tag{58}$$

in which r_0 is a point locating at the middle of the interphase layer and R_n are the coefficients of the power series.

Substituting Eq. (58) into Eq. (57) and using the Series Solution method yield

$$u_i^r(r) = R_0 f_1(r - r_0) + R_1 f_2(r - r_0) \tag{59}$$

where $f_1(r - r_0)$ and $f_2(r - r_0)$ are n orders polynomials with respect to $(r - r_0)$. The coefficients can be determined by the Taylor expansions of $p(r)$ and $q(r)$ (Johnson and Johnson, 1965). Numerical calculations show that the convergence of the solution is satisfied only if $n \geqslant 8$. Therefore, $n = 8$ is taken in Eq. (59) in order to get an asymptotic solution of u_i^r. The radial and hoop strains can be obtained as

$$\varepsilon_i^r = R_0 f_1' + R_1 f_2', \quad \varepsilon_i^\theta = R_0\frac{f_1}{r} + R_1\frac{f_2}{r} \tag{60}$$

f_1', f_2' are the derivatives of f_1, f_2 with respect to r. Meanwhile, the radial and hoop stresses in the interphase are

$$\sigma_i^{rp} = \frac{E_i}{I_i}[A_1(r)R_0 + A_2(r)R_1] + \frac{\nu_i}{1-\nu_i}\sigma_i$$
$$\sigma_i^{\theta p} = \frac{E_i}{I_i}[A_3(r)R_0 + A_4(r)R_1] + \frac{\nu_i}{1-\nu_i}\sigma_i \tag{61}$$
$$\sigma_i^{rp} + \sigma_i^{\theta p} = \frac{E_i}{I_i}[A_5(r)R_0 + A_6(r)R_1] + \frac{2\nu_i}{1-\nu_i}\sigma_i$$

where

$$A_1(r) = \eta\left(y_1' + \nu_i\frac{y_1}{r}\right), \quad A_2(r) = \eta\left(y_2' + \nu_i\frac{y_2}{r}\right),$$
$$A_3(r) = \eta\left(\nu_i y_1' + \frac{y_1}{r}\right), \quad A_4(r) = \eta\left(\nu_i y_2' + \frac{y_2}{r}\right), \tag{62}$$
$$A_5 = A_1 + A_3, \quad A_6 = A_2 + A_4$$
$$\eta = \frac{(1+\nu_i)(1-2\nu_i)}{1-\nu_i}$$

Using the boundary conditions in Eqs. (23)–(25) results in

$$\begin{cases} A = \frac{1}{H_4}(H_1\sigma_f + H_2\sigma_i + H_3\sigma_m) \\ R_0 = \frac{E_m F_4(S_1\sigma_i - \nu_f\sigma_f) - E_f F_2(S_2\sigma_i - \nu_m\sigma_m)}{E_m E_f(F_1F_4 - F_2F_3)} \\ R_1 = \frac{E_m F_3(S_1\sigma_i - \nu_f\sigma_f) - E_f F_1(S_2\sigma_i - \nu_m\sigma_m)}{E_m E_f(F_2F_3 - F_1F_4)} \\ F = -r_m^2 H \\ H = -\frac{r_i^2}{r_m^2 - r_i^2}\frac{1}{H_4}(H_5\sigma_f + H_6\sigma_i + H_7\sigma_m) \end{cases} \tag{63}$$

Further, we have

$$\left(\sigma_i^{rp} + \sigma_i^{\theta p}\right)_{r=r_f} = \frac{1}{H_4}(H_8\sigma_f + H_9\sigma_i + H_{10}\sigma_m)$$
$$\left(\sigma_i^{rp} + \sigma_i^{\theta p}\right)_{r=r_i} = \frac{1}{H_4}(H_{11}\sigma_f + H_{12}\sigma_i + H_{13}\sigma_m) \tag{64}$$

The parameters $F_1 \sim F_4$, $H_1 \sim H_{13}$, S_1 and S_2 in the above equations are given in Appendix B.

4.2. Thermal residual stress

In the homogeneous fiber and matrix, the radial displacements induced by the thermal effect possess similar forms to Eq. (28). The general solution of the radial displacement $\bar{u}_i^r$ can be obtained by the series solution method (Johnson and Johnson, 1965; Jayaraman and Reifsnider, 1992),

$$\bar{u}_i^r(r) = \bar{R}_0\bar{f}_1(r-r_0) + \bar{R}_1\bar{f}_2(r-r_0) - \nu_i\bar{D}r \tag{65}$$

Numerical calculations show that $n = 8$ can guarantee the convergence of the asymptotic solution of $\bar{u}_i^r$. Then the radial and hoop stresses in the interphase are

$$\begin{aligned} q_i^r &= \frac{E_i}{I_i}\left[\bar{A}_1(r)\bar{R}_0 + \bar{A}_2(r)\bar{R}_1\right] \\ q_i^\theta &= \frac{E_i}{I_i}\left[\bar{A}_3(r)\bar{R}_0 + \bar{A}_4(r)\bar{R}_1\right] \\ q_i^r + q_i^\theta &= \frac{E_i}{I_i}\left[\bar{A}_5(r)\bar{R}_0 + \bar{A}_6(r)\bar{R}_1\right] \end{aligned} \tag{66}$$

in which

$$\begin{aligned} &\bar{A}_1(r) = (1-\nu_i^2)\bar{y}_1' + \nu_i(1+\nu_i)\frac{\bar{y}_1}{r}, \quad \bar{A}_2(r) = (1-\nu_i^2)\bar{y}_2' + \nu_i(1+\nu_i)\frac{\bar{y}_2}{r}, \\ &\bar{A}_3(r) = (1-\nu_i^2)\frac{\bar{y}_1}{r} + \nu_i(1+\nu_i)\bar{y}_1', \quad \bar{A}_4(r) = (1-\nu_i^2)\frac{\bar{y}_2}{r} + \nu_i(1+\nu_i)\bar{y}_2', \\ &\bar{A}_5 = \bar{A}_1 + \bar{A}_3, \quad \bar{A}_6 = \bar{A}_2 + \bar{A}_4 \end{aligned} \tag{67}$$

Using the boundary conditions in Eqs. (32)–(35), we have

$$\begin{cases} \bar{A} = K_1\bar{D} + K_2q_1 + K_3q_2 \\ \bar{R}_0 = \frac{\bar{F}_4[q_1\Delta T + (\nu_i-\nu_f)\bar{D}] - \bar{F}_2[q_2\Delta T + (\nu_i-\nu_m)\bar{D}]}{\bar{F}_1\bar{F}_4 - \bar{F}_2\bar{F}_3} \\ \bar{R}_1 = \frac{\bar{F}_3[q_1\Delta T + (\nu_i-\nu_f)\bar{D}] - \bar{F}_1[q_2\Delta T + (\nu_i-\nu_m)\bar{D}]}{\bar{F}_2\bar{F}_3 - \bar{F}_1\bar{F}_4} \\ \bar{F} = K_4\bar{D} + K_5q_1 + K_6q_2 \\ \bar{H} = \frac{r_m^2}{1-2\nu_m}[(K_4+\nu_m)\bar{D} + K_5q_1 + K_6q_2] \\ \bar{D} = -\frac{1}{K_7}(K_8q_1 + K_9q_2) \end{cases} \tag{68}$$

where $q_1 = (\alpha_f - \alpha_i)\Delta T$, $q_2 = (\alpha_m - \alpha_i)\Delta T$. For the case with a linearly graded interphase, $q_\alpha^r + q_\alpha^\theta (\alpha = f, i, m)$ has the same general forms as Eq. (37), and the relevant parameters $K_1 \sim K_{15}, \bar{F}_1 \sim \bar{F}_4$ are given in Appendix B.

4.3. Stresses in the improved shear-lag model

Combining Eqs. (5), (13), (61) and (66) yields

$$\begin{aligned} \varepsilon_i^z(r,z) &= \frac{1}{E_i}\left[\sigma_i - \nu_i(\sigma_i^r + \sigma_i^\theta)\right] \\ &= \left(1 - \frac{2\nu_i^2}{1-\nu_i}\right)\frac{\sigma_i}{a+br} \\ &\quad - \frac{\nu_i}{I_i}\left[A_5(r)R_0 + A_6(r)R_1 + \bar{A}_5(r)\bar{R}_0 + \bar{A}_6(r)\bar{R}_1\right] \end{aligned} \tag{69}$$

Then, the integral in Eq. (8) can be written as

$$\begin{aligned} \int_{r_f}^{r_i} \frac{E_i}{2(1+\nu_i)}\frac{\partial\varepsilon_i^z(r,z)}{\partial r}dr = &-\frac{\ln(E_m/E_f)}{2(1+\nu_i)}\left(1 - \frac{2\nu_i^2}{1-\nu_i}\right)\sigma_i \\ &- \frac{\nu_i}{2I_i(1+\nu_i)}\int_{r_f}^{r_i}[A_7(r)R_0 + A_8(r)R_1 \\ &+ \bar{A}_7(r)\bar{R}_0 + \bar{A}_8(r)\bar{R}_1\Big]dr \end{aligned} \tag{70}$$

in which

$$\begin{aligned} A_7(r) &= (a+br)\frac{dA_5(r)}{dr}, \quad A_8(r) = (a+br)\frac{dA_6(r)}{dr}, \\ \bar{A}_7(r) &= (a+br)\frac{d\bar{A}_5(r)}{dr}, \quad \bar{A}_8(r) = (a+br)\frac{d\bar{A}_6(r)}{dr} \end{aligned} \tag{71}$$

Substituting $R_0, R_1, \bar{R}_0, \bar{R}_1$ into Eq. (70) yields

$$\begin{aligned} \int_{r_f}^{r_i} \frac{E_i}{2(1+\nu_i)}\frac{\partial\varepsilon_i^z(r,z)}{\partial r}dr = &-\left(1 - \frac{2\nu_i^2}{1-\nu_i}\right)\frac{\ln(E_m/E_f)}{2(1+\nu_i)}\sigma_i \\ &- \frac{\nu_i}{2I_i(1+\nu_i)}[C_1\sigma_f + C_2\sigma_i + C_3\sigma_m + Q_5] \end{aligned} \tag{72}$$

where $Q_5 = (C_5 - C_4\frac{K_8}{K_7})q_1 + \left(C_6 - C_4\frac{K_9}{K_7}\right)q_2$.

Combining Eqs. (5), (13), (14), (64) and (69) leads to another term in Eqs. (8) and (9),

$$\begin{aligned} \varepsilon_m(r_m,z) - \varepsilon_i(r_i,z) = &\frac{\nu_i}{E_i}Q_4 - \frac{\nu_m}{E_m}Q_2 \\ &+ \left[\frac{2\nu_m r_i^2}{E_m(r_m^2-r_i^2)}\frac{H_5}{H_4} + \frac{\nu_i}{E_i}\frac{H_{11}}{H_4}\right]\sigma_f \\ &+ \left[\frac{2\nu_m r_i^2}{E_m(r_m^2-r_i^2)}\frac{H_6}{H_4} - \frac{1}{E_i} + \frac{\nu_i}{E_i}\frac{H_{12}}{H_4}\right]\sigma_i \\ &+ \left[\frac{1}{E_m}\left(1 + \frac{2\nu_m r_i^2}{r_m^2-r_i^2}\frac{H_7}{H_4}\right) + \frac{\nu_i}{E_i}\frac{H_{13}}{H_4}\right]\sigma_m \end{aligned} \tag{73}$$

Then, we have

$$\begin{aligned} \frac{d\tau_1}{dz} &= \frac{1}{B_1r_f}(C_7\sigma_f + C_8\sigma_i + C_9\sigma_m + Q_6) \\ \frac{d\tau_2}{dz} &= \frac{1}{2(1+\nu_m)B_3r_i}(C_{10}\sigma_f + C_{11}\sigma_i + C_{12}\sigma_m + Q_7) \\ Q_6 &= -\frac{B_2}{2(1+\nu_m)B_3}\left(\nu_mQ_2 - \frac{E_m}{E_i}\nu_iQ_4\right) - \frac{\nu_i}{2I_i(1+\nu_i)}Q_5 \\ Q_7 &= -\nu_mQ_2 + \frac{E_m}{E_i}\nu_iQ_4 \end{aligned} \tag{74}$$

Similar to Section 3.3, we can finally obtain a fourth-order differential equation for fiber's axial stress σ_f, which has the same form as Eq. (49). Parameters $C_1 \sim C_{12}$ in this case are given in Appendix B.

5. Results and discussions

Consider a unidirectional carbon fiber-reinforced composite system subjected to a uniform tensile stress σ_0. The matrix is a brittle thermosetting polymer (e.g. epoxy resins), which enables the tensile load to be transferred by the elastic shear deformation at interfaces (Huang and Young, 1996; Leveque and Auvray, 1996). In the composite system, Young's modulus of the interphase varies continuously in the radial direction (Liu et al., 2008; Yang and Pitchumani, 2004). According to Chai and Mai (2001), Fu et al. (2000), Jayaraman and Reifsnider (1992), Kiritsi and Anifantis (2001), Wu et al. (1997) and Zhang et al. (2010), the material parameters are taken as: $E_f = 230$ GPa, $E_m = 5$ GPa, $\nu_f = 0.2$, $\nu_i = \nu_m = 0.35$, $\rho = 10$, $\alpha_f = 12 \times 10^{-6}/°C$, $\alpha_i = 28 \times 10^{-6}/°C$, $\alpha_m = 55 \times 10^{-6}/°C$, $\Delta T = -100$ °C. The ratio of length is $L_f/L_m = 0.5$, which will be fixed in the present paper. Then, the volume fraction of fibers in Eq. (1) depends only on the ratio r_f/r_m. Initially, we choose $V_f = 0.18$ and the uniform tensile load $\sigma_0 = 10$ MPa. Based on the above theoretical analysis, the effects of the inhomogeneous interphase on the mechanism of stress transfer among fibers, interphase and matrix are discussed as follows.

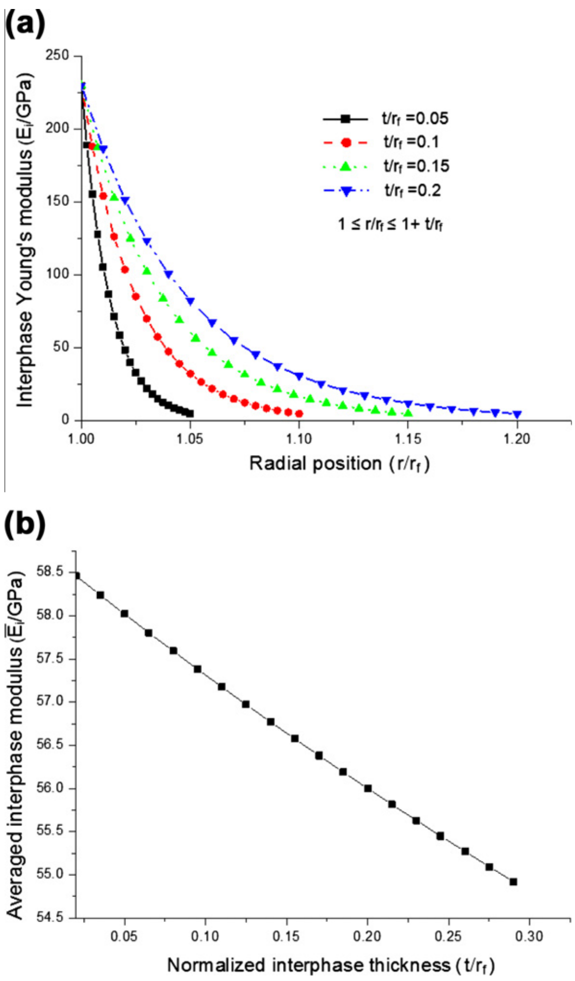

Fig. 3. (a) The interphase Young's modulus varying in the radial direction for different interphase thicknesses in the model with a power variation law; (b) The relation between the average interphase Young's modulus and the interphase thickness.

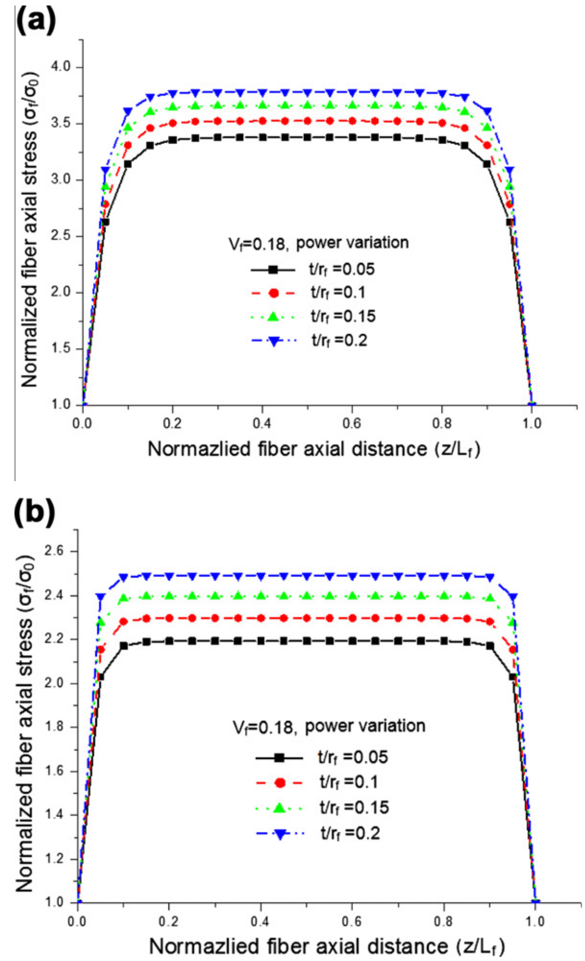

Fig. 4. Distributions of the fiber's axial stress along the axis of fibers for different interphase thicknesses in the model with a power variation law. (a) $V_f = 0.18$; (b) $V_f = 0.25$.

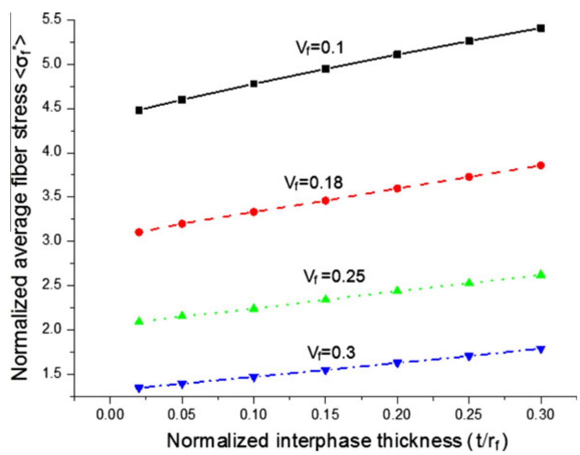

Fig. 5. The average fiber stress versus the interphase thickness for different volume fractions of fibers in the model with a power variation law.

5.1. The case with a power-graded interphase

Fig. 3(a) gives the Young's modulus of interphase E_i varying in the radial direction for different ratios of t/r_f according to a power variation law. Since the Young's modulus of fibers is much larger than that of matrix and the continuity conditions of Young's modulus at interfaces should be satisfied, E_i decreases in the radial direction. Fig. 3(b) shows the average Young's modulus of interphase as a function of the non-dimensional interphase thickness. From Fig. 3(b), one can see that $\overline{E}_i$ decreases slightly with an increasing interphase thickness. The thicker the interphase layer, the softer it will be. In this case, the overall modulus of the composite annulus surrounding the fiber will reduce as the volume fraction of interphase grows.

Fig. 4(a) and (b) plot distributions of the normalized fiber's axial stress along the normalized axial coordinate for cases with different interphase thicknesses and volume fractions of fibers. Clearly, the fiber's axial stress rises rapidly from two ends to reach a plateau value in cases with different volume fractions of fibers, and keeps almost uniform within the middle region of the fiber, exhibiting a similar pattern to those in Fu et al. (2000b), Wu et al. (1997) and Zhang and He (2008). Meanwhile, it is found that the increase of interphase thickness leads to an increase of fiber stress. This phenomenon can be explained by the reduction of the average interphase modulus with an increasing interphase thickness as shown in Fig. 3(b). Since the interphase layer becomes soft with an increasing interphase thickness, the effective stiffness of the composite annulus (formed by the matrix and interphase layers) surrounding the fiber decreases correspondingly, resulting in a weakened load bearing capacity of the materials outside the fiber. More external loads should be supported by the stiff carbon fiber. These results indicate that when the interphase modulus has a power variation, a thicker interphase layer is more helpful for a better stress transfer.

An average axial stress is defined as follows,

$$\left\langle \sigma_f^* \right\rangle = \int_0^1 \sigma_f^*(z^*)dz^* \tag{75}$$

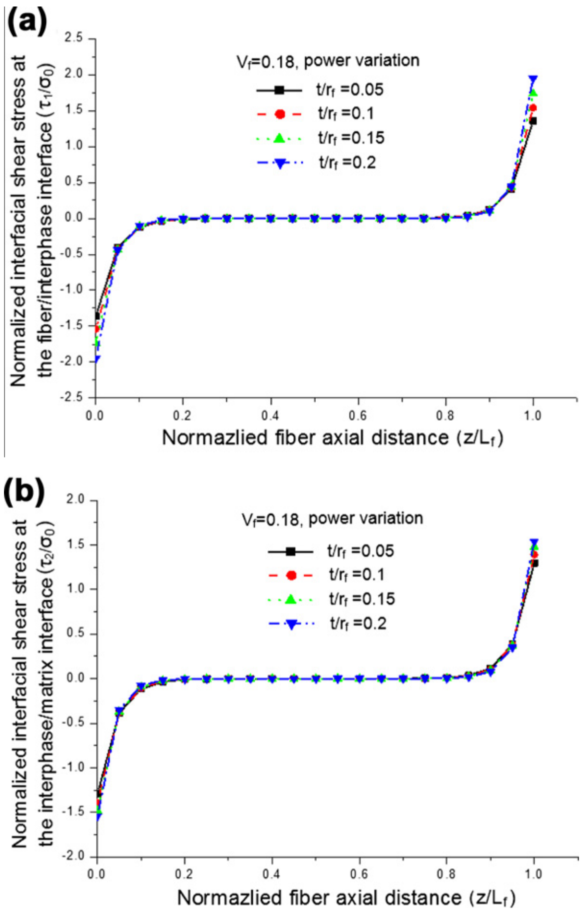

Fig. 6. Distributions of the interfacial shear stress along the axis of fibers for different interphase thicknesses in the model with a power variation law. (a) At the fiber/interphase interface; (b) At the interphase/matrix interface.

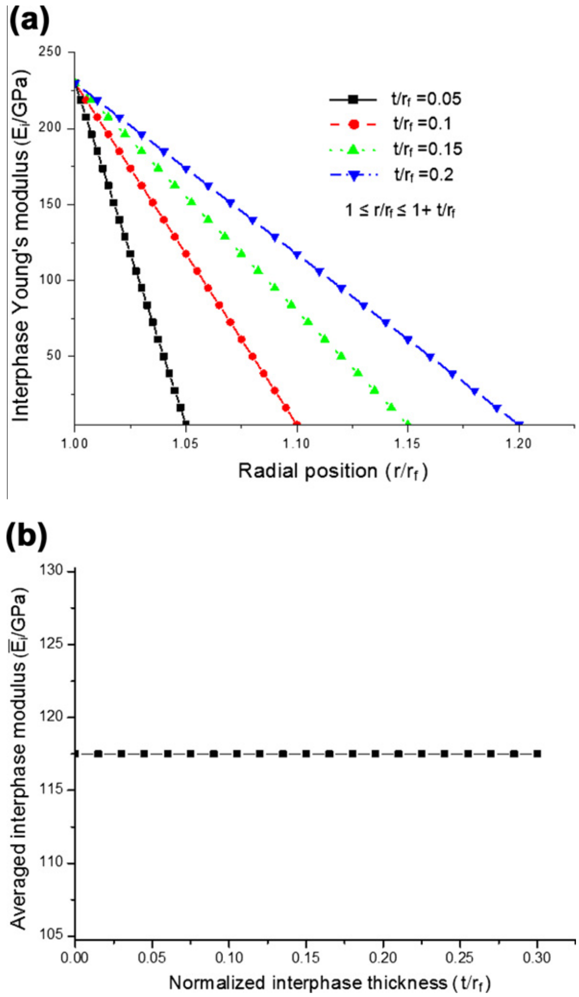

Fig. 7. (a) The interphase Young's modulus varying in the radial direction for different interphase thicknesses in the model with a linear variation law; (b) The relation between the average interphase modulus and the interphase thickness.

which is used to evaluate the stress level within the fiber. Fig. 5 gives the average axial stress as a function of interphase thickness for cases with different volume fractions of fibers. One can see that the average fiber stress increases almost linearly with an increasing interphase thickness, but with a low slope. This tendency is consistent well with that in Fig. 4. Both the results in Figs. 4 and 5 reveal that for the case with a power graded interphase, the fiber's axial stress will increase at a small and constant growth rate when the interphase zone becomes thicker. This argument is of significant reference for a proper design of interphase size to achieve a desirable axial stress of fibers.

Effects of the inhomogeneous interphase on the shear stresses τ_1 and τ_2 at the fiber/interphase and interphase/matrix interfaces are depicted in Fig. 6(a) and (b), respectively. It is found that not only the distribution of τ_1 but also that of τ_2 is almost insensitive to the variation of interphase thickness in the middle region of a fiber. This result is consistent with that in Fig. 4(a) and (b) and governed by the relations in Eq. (3), in which the interfacial shear stress depends only on the increment of the axial stress for a determined model structure. Only the interfacial shear

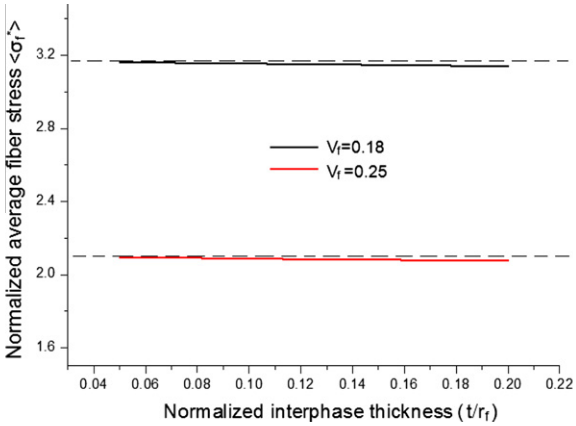

Fig. 9. The average fiber stress versus the interphase thickness for different volume fractions of fibers in the model with a linear variation law, the dashed line represents a referenced one parallel to the horizontal axis.

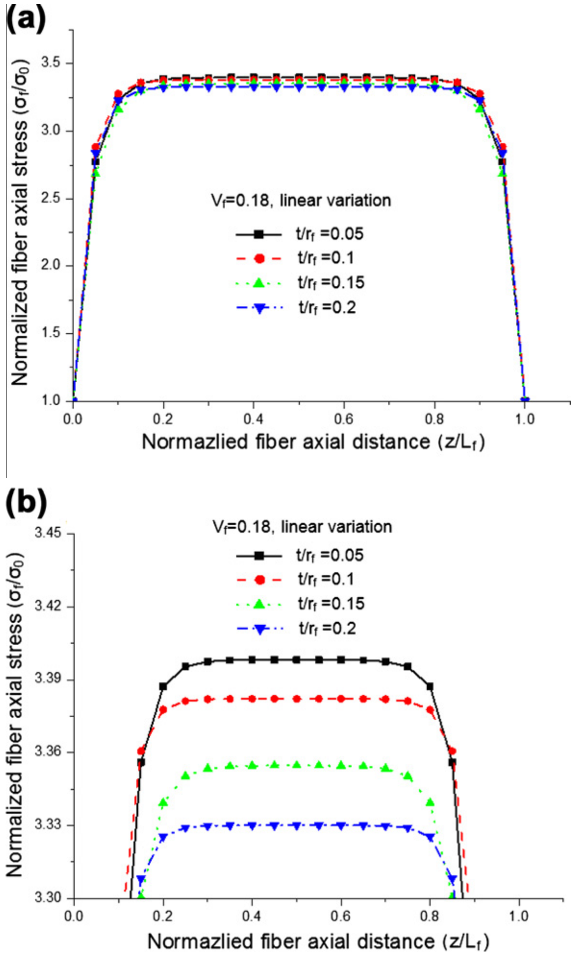

Fig. 8. Distributions of the fiber's axial stress along the axis of fibers for different interphase thicknesses in the model with a linear variation law: (a) The whole fiber length; (b) Amplifications of the middle region of the fiber ($0.1 \leqslant z/L \leqslant 0.9$).

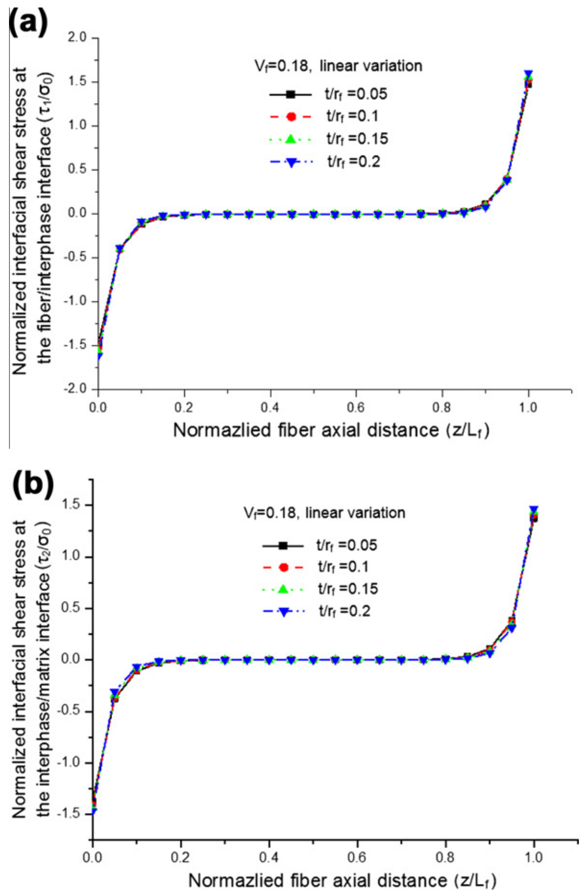

Fig. 10. Distributions of the interfacial shear stress along the axis of fibers for different interphase thicknesses in the model with a linear variation law. (a) At the fiber/interphase interface; (b) At the interphase/matrix interface.

stresses near both ends of the fiber are influenced by the interphase thickness.

5.2. The case with a linearly graded interphase

Fig. 7(a) gives the schematics of Young's modulus of the interphase varying in the radial direction with a linear feature. The continuity conditions lead to the linearly varying slope of the curves decreasing with an increasing interphase thickness. Fig. 7(b) shows the average Young's modulus of the interphase for cases with different interphase thicknesses. One can see that the average Young's modulus is a constant independent of the interphase thickness in the structure with a linear graded interphase.

Fig. 8(a) shows distributions of the normalized fiber stress along the axial direction for cases with different interphase thicknesses. In contrast to the corresponding results in the case with a power variation law as shown in Fig. 4(a), the interphase thickness does not exhibit significant effects on the distribution of the axial stress of fibers in the linear variation case. Amplifications of the axial stress distributions in the middle of fibers are shown in Fig. 8(b). It is surprising to find that, contrary to the results in Fig. 4(a), the plateau value decreases with an increasing interphase thickness, though the decrement is small. This feature is also reflected in Fig. 9, where the average fiber stress $\left\langle \sigma_f^* \right\rangle$ reduces linearly but slowly with an increasing interphase thickness. This phenomenon can also be characterized by the varying relation between the average interphase modulus and interphase thickness for the linear variation case, as shown in Fig. 7(b). It is noted that the volume fraction of the interphase in the cylindrical cell will increase and that of the matrix decreases with an increasing interphase thickness. The effective stiffness outside the carbon fiber is enhanced because the constant average interphase modulus $\overline{E}_i$ is much larger than the modulus of polymer matrix. Consequently, fibers share a less external load. With a constant average interphase modulus, the effects of interphase properties on stress transfer arise only from the variation of interphase thickness, which are actually very small (Fu et al., 2000b).

Comparing the results in Figs. 4 and 8, one can see that an increasing interphase thickness has totally opposite effects on the fiber stress in the cases with a power and a linear variation law. This phenomenon mainly arises from the different varying trends of the interphase effective stiffness versus thickness, as shown in Fig. 3(b) and 7(b), which is a distinct characteristic of the graded interphase as compared to a homogeneous one.

Effects of the interphase thickness on the shear stresses τ_1 and τ_2 at the fiber/interphase and interphase/matrix interfaces are depicted in Fig. 10(a) and (b), respectively. It is found that not only the distribution of τ_1 but also that of τ_2 is almost insensitive to the variation of interphase thickness in the middle region of a fiber. The result is very similar to that in the power variation case, which is governed by the relations in Eq. (3). The interfacial shear stress depends only on the increment of the axial stress for a determined model structure. Due to the existing plateaus in Fig. 8(a) and (b), the corresponding interfacial shear stress almost vanishes in the same region.

5.3. A comparison between the linear graded case and the power graded one

Fig. 11(a) and (b) show the distributions of axial stress of fibers for both cases with different volume fractions of fibers and different interphase thicknesses. In the case with a fixed interphase thickness, fiber's axial stress in the power case is larger than that in the linear one and it is reasonable to find that fiber's axial stress decreases with an increasing fiber's volume fraction. In the case with a fixed volume fraction of fibers, the difference of the fiber's axial stress between the power case and the linear one increases with an increasing interphase thickness. This tendency can also be explained from the perspective of the average interphase modulus. Since the average Young's modulus $\overline{E}_i$ in the power case is much smaller than that in the linear one, which leads to a softer stiffness outside the carbon fiber, the fiber in the former should sustain more tensile loads. On the other hand, the average Young's modulus $\overline{E}_i$ in the power law case decreases with an increasing interphase thickness, while $\overline{E}_i$ in the linear one keeps a constant.

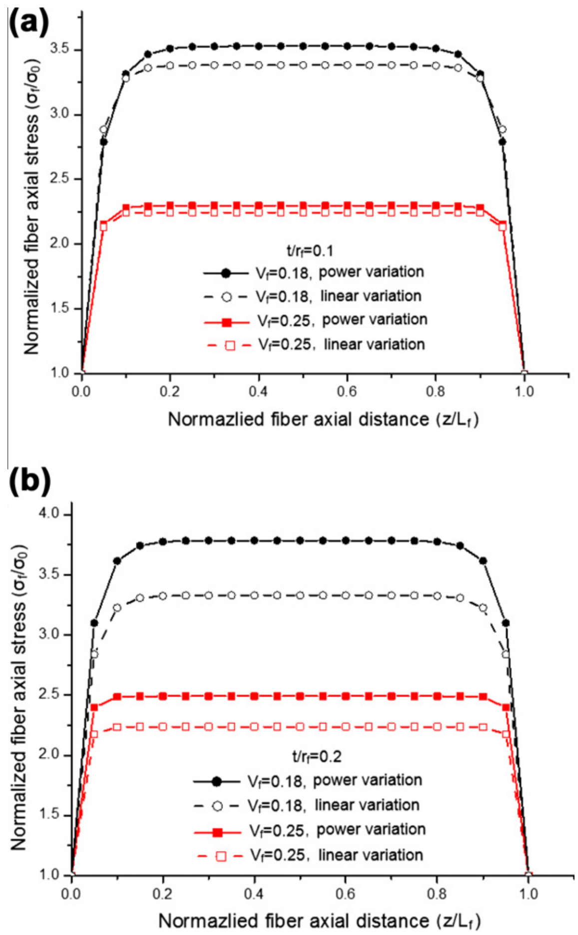

Fig. 11. Comparisons of the fiber's axial stress distributions between the case with a power variation law and that with a linear one. (a) For $t^* = 0.1$; (b) For $t^* = 0.2$.

Therefore, the deviation of fiber's axial stress in the two cases enlarges with an increasing interphase thickness. The results indicate that interphase with a power variation law should be more effective for stress transfer than that with a linear one.

Fig. 12(a)–(d) show the comparisons of the interfacial shear stresses for the power and linear variation cases. The differences between the two cases are very small if the interphase thickness is small, because the interfacial shear stresses τ_1 and τ_2 in most areas of the interface are almost insensitive to the interphase properties. Only when the interphase thickness becomes large, the interfacial shear stresses in the power variation case exceed those in the linear one at the region near the two ends of fibers.

In the practical design of novel fiber-reinforced composites, one of the main objectives is to prevent the interphase region from shear failure. The maximum shear stress in the interphase can be expressed as

$$\tau_i^{rz}(r,z) = \frac{1}{r_i^2 - r_f^2}\left[\left(\frac{r_i^2}{r} - r\right) r_f \tau_1(z) + \left(r - \frac{r_f^2}{r}\right) r_i \tau_2(z)\right], \quad (r_f \leqslant r \leqslant r_i) \tag{76}$$

At an arbitrary radial position, the distribution of τ_i^{rz} in z direction has the same characteristic as τ_1 and τ_2, so the maximum value should occur near the two ends of fiber,

$$\tau_{i\max}(r) = \left|\tau_i^{rz}(r,0)\right| = \frac{1}{r_i^2 - r_f^2}\left[\left(\frac{r_i^2}{r} - r\right) r_f |\tau_1(0)| + \left(r - \frac{r_f^2}{r}\right) r_i |\tau_2(0)|\right], \quad (r_f \leqslant r \leqslant r_i) \tag{77}$$

The distributions of $\tau_{i\ \max}$ for the two variation cases are shown in Fig. 13. The maximum shear stress $\tau_{i\ \max}$ is obviously larger in the power variation case than that in the linear one, which means that the latter should be more favorable for reducing stress concentration in the interphase region. Therefore, composites with an inhomogeneous interphase varying according to different laws may own their special purposes. The interphase with its Young's modulus varying according to a power law should be more efficient for stress transfer, while the one with a linear variation law is more advantageous in preventing shear fracture.

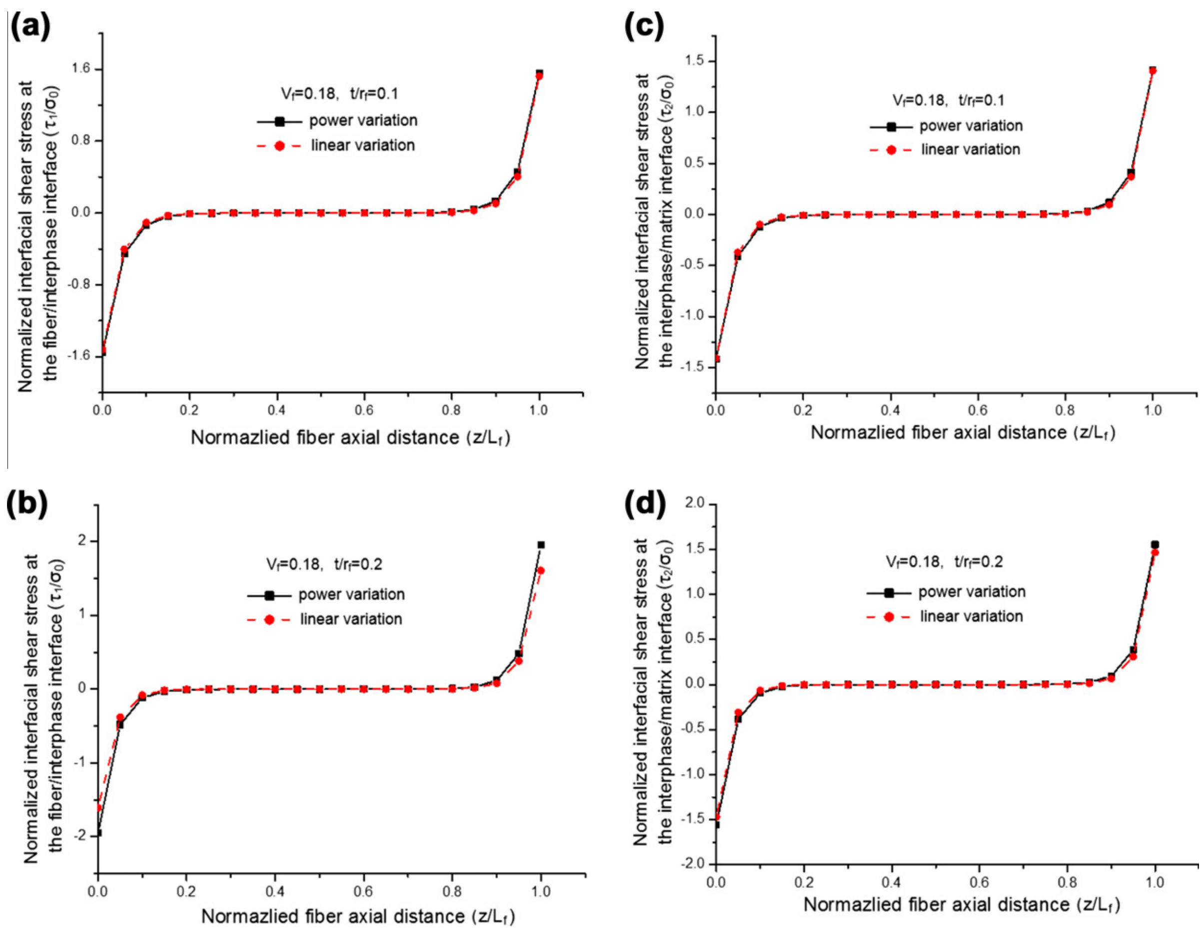

Fig. 12. Comparisons of the interfacial shear stress distributions between the case with a power variation law and that with a linear one. (a) At the fiber/interphase interface with $t^* = 0.1$; (b) At the fiber/interphase interface with $t^* = 0.2$; (c) At the interphase/matrix interface with $t^* = 0.1$; (d) At the interphase/matrix interface with $t^* = 0.2$.

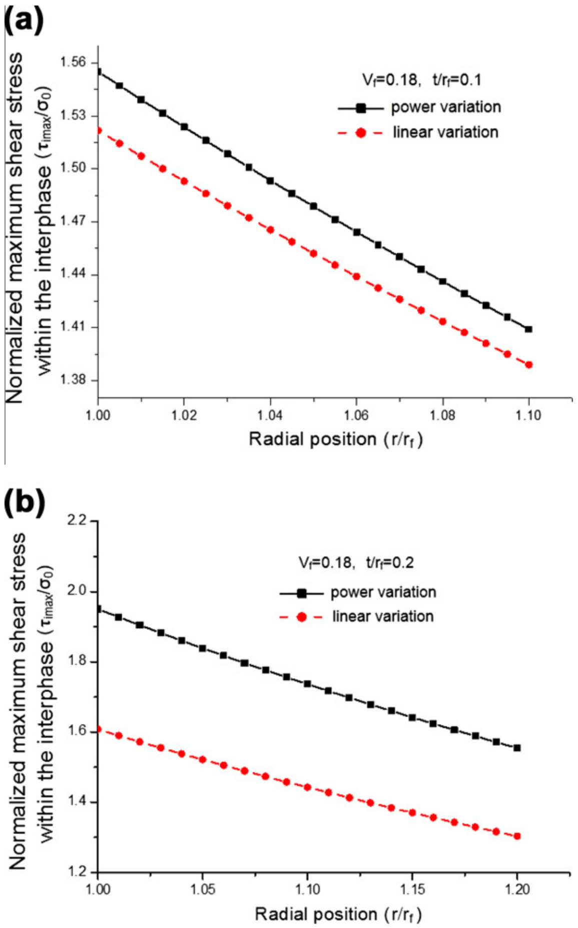

Fig. 13. Comparisons of the maximum shear stress in the interphase between the case with a power variation law and that with a linear one. (a) For $t^* = 0.1$; (b) For $t^* = 0.2$.

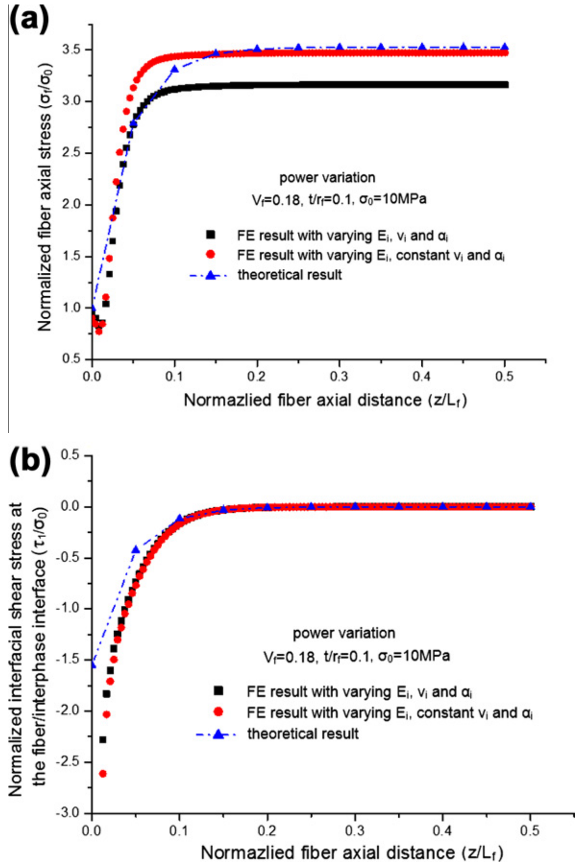

Fig. 14. Comparisons between the analytical and numerical predictions of the (a) Fiber stress and (b) Interfacial shear stress, for the case with a power variation law.

5.4. Finite element (FE) validation

To validate the analytical results, finite element calculations are carried out based on the three-phase composite system shown in Fig. 1. In order to simulate the thermal residual stresses in different phases, the composite system is subjected to a temperature change ΔT. ABAQUS is used as a solver (DS SIMULIA, 2010) and the graded feature of the interphase properties are implemented into the numerical model via the subroutine USDFLD available in ABAQUS.

Fig. 14(a) illustrates the theoretical and numerical predictions of fiber's axial stress for the case with a power-graded interphase. It is found that the theoretical result agrees well with the numerical one in the case that the interphase has a power-graded Young's modulus, but a constant Poisson's ratio and a constant thermal expansion coefficient. If not only the Young's modulus but also the Poisson's ratio and thermal expansion coefficient vary according to the same power-graded law as given by Eq. (10) in the radial direction, the numerical result for this case will have a small difference from the theoretical result with assumptions of constant Poisson's ratio and thermal expansion coefficient, but the deviation is less than 10%. Fig. 14(b) gives the theoretical and numerical predictions of the fiber/interphase interfacial shear stress, in which one can see that the interfacial shear stress is hardly sensitive to the power graded Poisson's ratio and thermal expansion coefficient in the interphase.

Fig. 15(a) and (b) present the analytical and numerical results for the case with a linearly graded interphase. One can see that the effects of the linearly graded Poisson's ratio and thermal expansion coefficient of the interphase on the fiber's axial stress and interfacial shear stress at the fiber/interphase interface are very weak. The deviation between the theoretical prediction and the numerical one is less than 10%.

The above comparisons demonstrate that the spatial variations of the interphase Poisson's ratio and thermal expansion coefficient have very limited influences on the stress distributions in the three-phase composite system, and the constant assumptions of Poisson's ratio and thermal expansion coefficient in our analytical model is reasonable. In fact, the constant assumptions have been adopted in many studies of elastic graded materials, such as Chen et al. (2009), Giannakopoulos and Pallot (2000), Jayaraman and Reifsnider (1992) and Suresh et al. (1997).

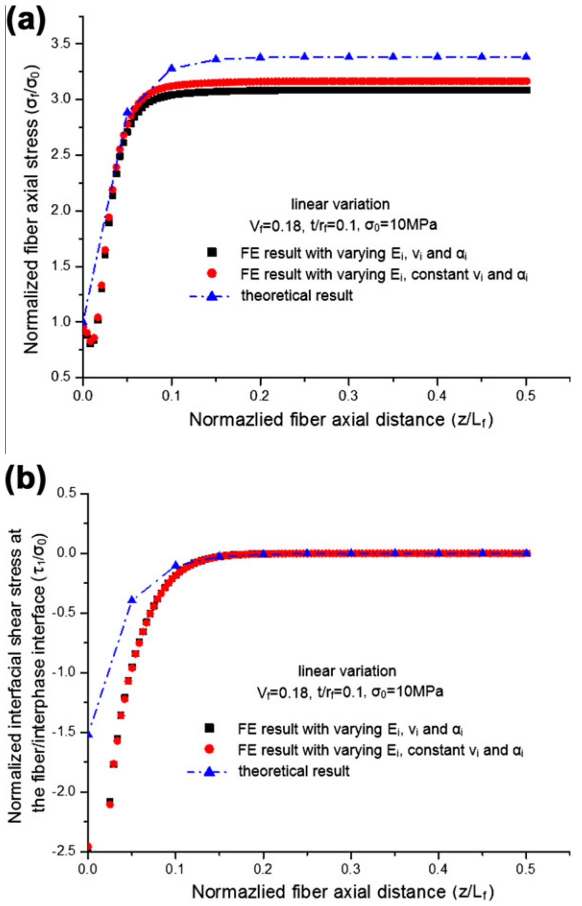

Fig. 15. Comparisons between the analytical and numerical predictions of the (a) Fiber stress and (b) Interfacial shear stress, for the case with a linear variation law.

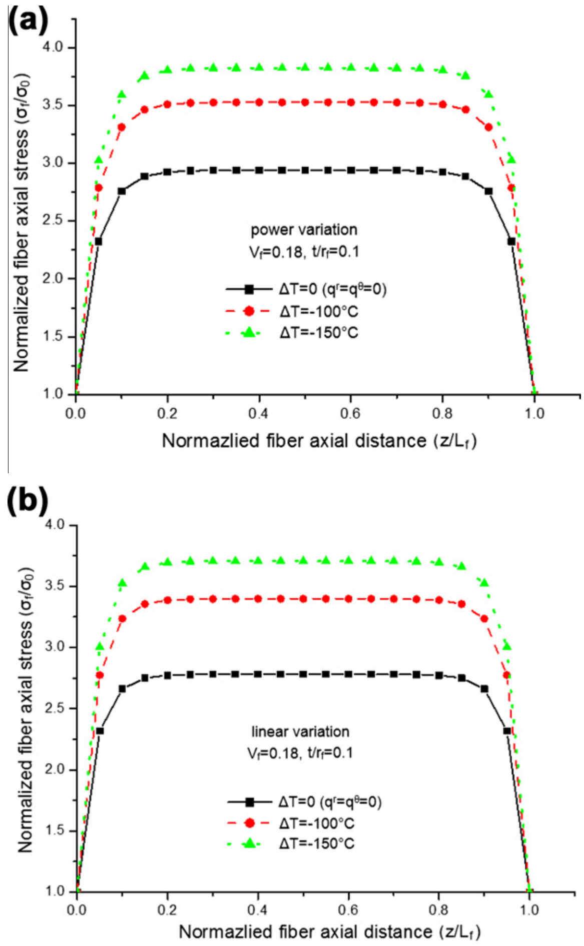

Fig. 16. Distributions of fiber stress under different temperature changes for (a) A power-graded interphase; (b) A linearly graded interphase.

5.5. Effects of thermal mismatch on the stress transfer

The thermal expansion coefficients of different phases are taken to be constants in our model, the magnitude of thermal residual stress is governed by the temperature change ΔT during the fabrication of composites. The distributions of fiber stress under different ΔT are shown in Fig. 16(a) and (b) for cases with a power and linearly graded interphase, respectively. It is easy to find that the fiber stress increases with an increasing ΔT, which is qualitatively consistent with the numerical results in Song et al. (1996) and the experimental results in Huang and Young (1996). Due to the increasing thermal mismatch, the radial pressure at the interface increases, resulting in an increasing fiber's axial stress owing to the Poisson's effect.

Fig. 17 gives the corresponding distributions of interfacial shear stress under different ΔT for the two cases. The interfacial shear stress increases slightly near the two ends of fibers with an increasing ΔT, which was also evidenced by Huang and Young (1996) and Song et al. (1996). Therefore, thermal mismatch in such a three-phase composite would be helpful for achieving a better stress transfer, but has a negative effect on protecting interface from shear failure.

6. Conclusions

A three-phase shear-lag model is developed in this paper to investigate the effects of an inhomogeneous interphase on the mechanism of stress transfer in unidirectional fiber-reinforced composites. The interphase Young's modulus is regarded as spatially non-uniform while other material parameters are chosen to be constant. A power variation law and a linear one of interphase Young's modulus are considered, respectively. Closed-form solutions to the fiber's axial stress and interfacial shear stress are obtained. In the former, it is interesting to find that the increase of interphase thickness leads to an increasing fiber's axial stress due to the reduction of the effective stiffness of a thickened interphase layer. In the latter, the fiber's axial stress is found to decrease with an increasing interphase thickness due to the enhancing overall modulus of the composite materials outside fibers. In both cases, the

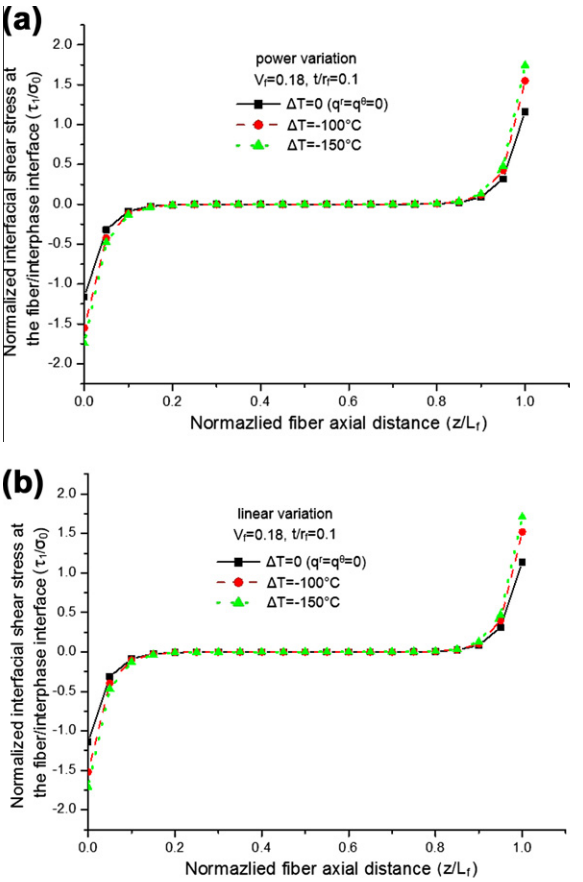

Fig. 17. Distributions of interfacial shear stress under different temperature changes for (a) A power-graded interphase; (b) A linearly graded interphase.

interfacial shear stress is almost insensitive to the interphase thickness except that near the two ends of fibers. All the phenomena can be characterized by an average Young's modulus of interphase, which reduces or keeps invariant in the two cases, respectively. Moreover, comparisons of both cases show that the former one is more advantageous in stress transfer, while the latter is more favorable for preventing shear failure. Numerical calculations are carried out and the numerical results agree with the theoretical ones, which demonstrates the reasonability of the constant assumptions of Poisson's ratio and thermal expansion coefficient of the interphase. The results in the present paper are derived based on the elastic load transfer mechanism, which should be useful for the design of some novel fiber-reinforced thermosetting matrix composites, especially for those with a modified interphase due to a weakly adhesive interface between the fiber and matrix, such as carbon fiber-reinforced epoxy composites

Acknowledgments

The work reported here is supported by NSFC through Grants #10972220, #11125211, #11021262 and Nano 973 Project (#2012CB937500).

Appendix A

In the case with the Young's modulus of interphase varying according to a power graded law, $F_1 \sim F_4$, S_1, S_2 in Eq. (26) are

$$\begin{aligned}
&F_1 = 1 - \frac{1-v_f}{I_i} A_1, \quad F_2 = 1 - \frac{1-v_f}{I_i} A_2, \\
&F_3 = 1 + \frac{(1+v_m^2) r_m^2 + (1-v_m) r_i^2}{r_m^2 - r_i^2} \frac{A_1}{I_i}, \\
&F_4 = 1 + \frac{(1+v_m^2) r_m^2 + (1-v_m) r_i^2}{r_m^2 - r_i^2} \frac{A_2}{I_i}, \\
&S_1 = \frac{v_i}{1-v_i}(1-v_f), \quad S_2 = -\frac{v_i}{1-v_i} \frac{(1+v_m^2) r_m^2 + (1-v_m) r_i^2}{r_m^2 - r_i^2}
\end{aligned} \tag{A.1}$$

Then, $H_1 \sim H_{14}$ in Eqs. (26) and (29) can be expressed as

$$\begin{aligned}
&H_1 = \frac{v_f}{I_i}\left[A_2F_3\left(\frac{r_i}{r_f}\right)^{m_1-1} - A_1F_4\left(\frac{r_i}{r_f}\right)^{m_2-1}\right] \\
&H_2 = \frac{1}{I_i}\left[A_1F_4S_1\left(\frac{r_i}{r_f}\right)^{m_2-1} - \frac{E_f}{E_m}A_1F_2S_2 + \frac{E_f}{E_m}A_2F_1S_2 - A_2F_3S_1\left(\frac{r_i}{r_f}\right)^{m_1-1}\right] + \frac{H_4 v_i}{1-v_i} \\
&H_3 = \frac{v_m E_f}{I_i E_m}(A_1F_2 - A_2F_1), \quad H_4 = E_f\left[\left(\frac{r_i}{r_f}\right)^{m_2-1} F_1F_4 - \left(\frac{r_i}{r_f}\right)^{m_1-1} F_2F_3\right] \\
&H_5 = \frac{v_f E_m}{I_i E_f}\left(\frac{r_i}{r_f}\right)^{m_2-1}(A_2F_3 - A_1F_4) \\
&H_6 = \frac{E_m}{I_i E_f}\left[A_1F_4S_1\left(\frac{r_i}{r_f}\right)^{m_2-1} - \frac{E_f}{E_m}A_1F_2S_2 + \frac{E_f}{E_m}A_2F_1S_2\left(\frac{r_i}{r_f}\right)^{m_2-m_1} - A_2F_3S_1\left(\frac{r_i}{r_f}\right)^{m_2-1}\right] + \frac{H_8 v_i}{1-v_i} \\
&H_7 = \frac{v_m}{I_i}\left[A_1F_2 - A_2F_1\left(\frac{r_i}{r_f}\right)^{m_2-m_1}\right], \quad H_8 = \left(\frac{r_i}{r_f}\right)^{m_2-m_1} F_1F_4 - F_2F_3 \\
&H_9 = \frac{v_f}{I_i}\left[A_6F_3\left(\frac{r_i}{r_f}\right)^{m_1-1} - A_5F_4\left(\frac{r_i}{r_f}\right)^{m_2-1}\right] \\
&H_{10} = \frac{1}{I_i}\left[A_5F_4S_1\left(\frac{r_i}{r_f}\right)^{m_2-1} - \frac{E_f}{E_m}A_5F_2S_2 + \frac{E_f}{E_m}A_6F_1S_2 - A_6F_3S_1\left(\frac{r_i}{r_f}\right)^{m_1-1}\right] + \frac{2H_4 v_i}{1-v_i} \\
&H_{11} = \frac{v_m E_f}{I_i E_m}[A_5F_2 - A_6F_1], \quad H_{12} = \frac{v_f E_m}{I_i E_f}\left(\frac{r_i}{r_f}\right)^{m_2-1}(A_6F_3 - A_5F_4) \\
&H_{13} = \frac{E_m}{I_i E_f}\left[A_5F_4S_1\left(\frac{r_i}{r_f}\right)^{m_2-1} - \frac{E_f}{E_m}A_5F_2S_2 + \frac{E_f}{E_m}A_6F_1S_2\left(\frac{r_i}{r_f}\right)^{m_2-m_1} - A_6F_3S_1\left(\frac{r_i}{r_f}\right)^{m_2-1}\right] + \frac{2H_8 v_i}{1-v_i} \\
&H_{14} = \frac{v_m}{I_i}\left[A_5F_2 - A_6F_1\left(\frac{r_i}{r_f}\right)^{m_2-m_1}\right]
\end{aligned} \tag{A.2}$$

The parameters A_1, A_2, A_5, A_6 in Eqs. (A.1) and (A.2) can be found in Eq. (22).

In the part of thermal residual stress, the coefficients $\overline{F}_1 \sim \overline{F}_4$ in Eq. (36) are

$$\begin{aligned}
&\overline{F}_1 = 1 - \frac{I_f}{I_i(1+v_f)}\overline{A}_1, \overline{F}_2 = 1 - \frac{I_f}{I_i(1+v_f)}\overline{A}_2, \\
&\overline{F}_3 = 1 + \frac{I_m\overline{A}_1}{I_i(1+v_m)}\left[\frac{r_i^2}{r_m^2 - r_i^2} + \frac{r_m^2}{(1-2v_m)(r_m^2 - r_i^2)}\right] \\
&\overline{F}_4 = 1 + \frac{I_m\overline{A}_2}{I_i(1+v_m)}\left[\frac{r_i^2}{r_m^2 - r_i^2} + \frac{r_m^2}{(1-2v_m)(r_m^2 - r_i^2)}\right]
\end{aligned} \tag{A.3}$$

Then the coefficients $K_1 \sim K_9$ in Eq. (36) can be expressed as

$$K_1 = \frac{I_f}{I_i(1+v_f)} \frac{\overline{A}_1\overline{F}_4(v_i - v_f)\left(\frac{r_i}{r_f}\right)^{\bar{m}_2-1} - \overline{A}_2\overline{F}_3(v_i - v_f)\left(\frac{r_i}{r_f}\right)^{\bar{m}_1-1} + (\overline{A}_2\overline{F}_1 - \overline{A}_1\overline{F}_2)(v_i - v_m)}{\overline{F}_1\overline{F}_4\left(\frac{r_i}{r_f}\right)^{\bar{m}_2-1} - \overline{F}_2\overline{F}_3\left(\frac{r_i}{r_f}\right)^{\bar{m}_1-1}} - v_f$$

$$K_2 = \frac{I_f}{I_i(1+v_f)} \frac{\overline{A}_1\overline{F}_4\left(\frac{r_i}{r_f}\right)^{\bar{m}_2-1} - \overline{A}_2\overline{F}_3\left(\frac{r_i}{r_f}\right)^{\bar{m}_1-1}}{\overline{F}_1\overline{F}_4\left(\frac{r_i}{r_f}\right)^{\bar{m}_2-1} - \overline{F}_2\overline{F}_3\left(\frac{r_i}{r_f}\right)^{\bar{m}_1-1}}, \quad K_3 = \frac{-I_f}{I_i(1+v_f)} \frac{\overline{A}_1\overline{F}_2 - \overline{A}_2\overline{F}_1}{\overline{F}_1\overline{F}_4\left(\frac{r_i}{r_f}\right)^{\bar{m}_2-1} - \overline{F}_2\overline{F}_3\left(\frac{r_i}{r_f}\right)^{\bar{m}_1-1}}$$

$$K_4 = -\frac{I_m r_i^2}{I_i} \frac{(\overline{A}_1\overline{F}_4 - \overline{A}_2\overline{F}_3)(v_i - v_f)\left(\frac{r_i}{r_f}\right)^{\bar{m}_2-1} + \left[\overline{A}_2\overline{F}_1\left(\frac{r_i}{r_f}\right)^{\bar{m}_2-\bar{m}_1} - \overline{A}_1\overline{F}_2\right](v_i - v_m)}{(r_m^2 - r_i^2)(1+v_m)[\overline{F}_1\overline{F}_4\left(\frac{r_i}{r_f}\right)^{\bar{m}_2-\bar{m}_1} - \overline{F}_2\overline{F}_3]} - v_m$$

$$\begin{aligned}K_5&=-\frac{I_m r_i^2}{I_i}\frac{(\overline{A}_1\overline{F}_4-\overline{A}_2\overline{F}_3)\left(\frac{r_i}{r_f}\right)^{\bar{m}_2-1}}{(r_m^2-r_i^2)(1+v_m)\left[\overline{F}_1\overline{F}_4\left(\frac{r_i}{r_f}\right)^{\bar{m}_2-\bar{m}_1}-\overline{F}_2\overline{F}_3\right]}K_6\\
&=-\frac{I_m r_i^2}{I_i}\frac{\overline{A}_2\overline{F}_1\left(\frac{r_i}{r_f}\right)^{\bar{m}_2-\bar{m}_1}-\overline{A}_1\overline{F}_2}{(r_m^2-r_i^2)(1+v_m)\left[\overline{F}_1\overline{F}_4\left(\frac{r_i}{r_f}\right)^{\bar{m}_2-\bar{m}_1}-\overline{F}_2\overline{F}_3\right]}K_7\\
&=\frac{E_f r_f^2}{2E_m I_f}\left[(1-v_f^2)+2v_f(1+v_f)K_1\right]+\frac{r_m^2-r_i^2}{2I_m}\left[(1-v_m^2)+2v_m(1+v_m)K_4\right]\\
&\quad+\frac{E_f M_1}{E_m}K_8\\
&=\frac{E_f v_f r_f^2}{E_m I_f}(1+v_f)K_2+\frac{r_m^2-r_i^2}{I_m}v_m(1+v_m)K_5+\frac{E_f M_2}{E_m}K_9\\
&=\frac{E_f v_f r_f^2}{E_m I_f}(1+v_f)K_3+\frac{r_m^2-r_i^2}{I_m}v_m(1+v_m)K_6+\frac{E_f M_3}{E_m}\end{aligned}\tag{A.4}$$

in which the parameters M_1, M_2, M_3 are

$$\begin{aligned}M_1&=\frac{1}{Q+2}\left[r_i^2\left(\frac{r_i}{r_f}\right)^{Q}-r_f^2\right]\\
&\quad+\frac{v_i(1+v_i)}{I_i}\left\{\frac{\bar{m}_1+1}{1-\bar{m}_2}\left[r_i^2\left(\frac{r_i}{r_f}\right)^{-(1+\bar{m}_2)}-r_f^2\right]\right.\\
&\quad\times\frac{\overline{F}_4\left(\frac{r_i}{r_f}\right)^{\bar{m}_2-1}(v_i-v_f)-\overline{F}_2(v_i-v_m)}{\overline{F}_1\overline{F}_4\left(\frac{r_i}{r_f}\right)^{\bar{m}_2-1}-\overline{F}_2\overline{F}_3\left(\frac{r_i}{r_f}\right)^{\bar{m}_1-1}}-\frac{\bar{m}_2+1}{1-\bar{m}_1}\\
&\quad\left.\times\left[r_i^2\left(\frac{r_i}{r_f}\right)^{-(1+\bar{m}_1)}-r_f^2\right]\frac{\overline{F}_3\left(\frac{r_i}{r_f}\right)^{\bar{m}_1-1}(v_i-v_f)-\overline{F}_1(v_i-v_m)}{\overline{F}_1\overline{F}_4\left(\frac{r_i}{r_f}\right)^{\bar{m}_2-1}-\overline{F}_2\overline{F}_3\left(\frac{r_i}{r_f}\right)^{\bar{m}_1-1}}\right\}\end{aligned}\tag{A.5}$$

$$\begin{aligned}M_2&=\frac{v_i(1+v_i)}{I_i}\left\{\frac{\bar{m}_1+1}{1-\bar{m}_2}\left[r_i^2\left(\frac{r_i}{r_f}\right)^{-(1+\bar{m}_2)}-r_f^2\right]\right.\\
&\quad\times\frac{\overline{F}_4\left(\frac{r_i}{r_f}\right)^{\bar{m}_2-1}}{\overline{F}_1\overline{F}_4\left(\frac{r_i}{r_f}\right)^{\bar{m}_2-1}-\overline{F}_2\overline{F}_3\left(\frac{r_i}{r_f}\right)^{\bar{m}_1-1}}-\frac{\bar{m}_2+1}{1-\bar{m}_1}\left[r_i^2\left(\frac{r_i}{r_f}\right)^{-(1+\bar{m}_1)}-r_f^2\right]\\
&\quad\left.\times\frac{\overline{F}_3\left(\frac{r_i}{r_f}\right)^{\bar{m}_1-1}}{\overline{F}_1\overline{F}_4\left(\frac{r_i}{r_f}\right)^{\bar{m}_2-1}-\overline{F}_2\overline{F}_3\left(\frac{r_i}{r_f}\right)^{\bar{m}_1-1}}\right\}\end{aligned}\tag{A.6}$$

$$\begin{aligned}M_3&=\frac{v_i(1+v_i)}{I_i}\left\{\frac{\bar{m}_1+1}{1-\bar{m}_2}\left[r_i^2\left(\frac{r_i}{r_f}\right)^{-(1+\bar{m}_2)}-r_f^2\right]\right.\\
&\quad\times\frac{-\overline{F}_2}{\overline{F}_1\overline{F}_4\left(\frac{r_i}{r_f}\right)^{\bar{m}_2-1}-\overline{F}_2\overline{F}_3\left(\frac{r_i}{r_f}\right)^{\bar{m}_1-1}}+\frac{\bar{m}_2+1}{1-\bar{m}_1}\left[r_i^2\left(\frac{r_i}{r_f}\right)^{-(1+\bar{m}_1)}-r_f^2\right]\\
&\quad\left.\times\frac{\overline{F}_1}{\overline{F}_1\overline{F}_4\left(\frac{r_i}{r_f}\right)^{\bar{m}_2-1}-\overline{F}_2\overline{F}_3\left(\frac{r_i}{r_f}\right)^{\bar{m}_1-1}}\right\}\end{aligned}\tag{A.7}$$

The coefficients $K_{10}\sim K_{15}$ in Eq. (37) are as follows,

$$K_{10}=\frac{E_f}{I_i}\frac{\overline{A}_5\overline{F}_4(v_i-v_f)\left(\frac{r_i}{r_f}\right)^{\bar{m}_2-1}-\overline{A}_6\overline{F}_3(v_i-v_f)\left(\frac{r_i}{r_f}\right)^{\bar{m}_1-1}+(\overline{A}_6\overline{F}_1-\overline{A}_5\overline{F}_2)(v_i-v_m)}{\overline{F}_1\overline{F}_4\left(\frac{r_i}{r_f}\right)^{\bar{m}_2-1}-\overline{F}_2\overline{F}_3\left(\frac{r_i}{r_f}\right)^{\bar{m}_1-1}}$$

$$K_{11}=\frac{E_f}{I_i}\frac{\overline{A}_5\overline{F}_4\left(\frac{r_i}{r_f}\right)^{\bar{m}_2-1}-\overline{A}_6\overline{F}_3\left(\frac{r_i}{r_f}\right)^{\bar{m}_1-1}}{\overline{F}_1\overline{F}_4\left(\frac{r_i}{r_f}\right)^{\bar{m}_2-1}-\overline{F}_2\overline{F}_3\left(\frac{r_i}{r_f}\right)^{\bar{m}_1-1}},\quad K_{12}=\frac{-E_f}{I_i}\frac{\overline{A}_5\overline{F}_2-\overline{A}_6\overline{F}_1}{\overline{F}_1\overline{F}_4\left(\frac{r_i}{r_f}\right)^{\bar{m}_2-1}-\overline{F}_2\overline{F}_3\left(\frac{r_i}{r_f}\right)^{\bar{m}_1-1}}$$

$$K_{13}=\frac{E_m}{I_i}\frac{(\overline{A}_5\overline{F}_4-\overline{A}_6\overline{F}_3)(v_i-v_f)\left(\frac{r_i}{r_f}\right)^{\bar{m}_2-1}+\left[\overline{A}_6\overline{F}_1\left(\frac{r_i}{r_f}\right)^{\bar{m}_2-\bar{m}_1}-\overline{A}_5\overline{F}_2\right](v_i-v_m)}{\overline{F}_1\overline{F}_4\left(\frac{r_i}{r_f}\right)^{\bar{m}_2-\bar{m}_1}-\overline{F}_2\overline{F}_3}$$

$$K_{14}=\frac{E_m}{I_i}\frac{(\overline{A}_5\overline{F}_4-\overline{A}_6\overline{F}_3)\left(\frac{r_i}{r_f}\right)^{\bar{m}_2-1}}{\overline{F}_1\overline{F}_4\left(\frac{r_i}{r_f}\right)^{\bar{m}_2-\bar{m}_1}-\overline{F}_2\overline{F}_3},\quad K_{15}=\frac{E_m}{I_i}\frac{\overline{A}_6\overline{F}_1\left(\frac{r_i}{r_f}\right)^{\bar{m}_2-\bar{m}_1}-\overline{A}_5\overline{F}_2}{\overline{F}_1\overline{F}_4\left(\frac{r_i}{r_f}\right)^{\bar{m}_2-\bar{m}_1}-\overline{F}_2\overline{F}_3}\tag{A.8}$$

The parameters $\overline{A}_1,\overline{A}_2,\overline{A}_5,\overline{A}_6$ in Eqs. (A.3), (A.4), (A.5), (A.6), (A.7), (A.8) can be found in Eq. (31).

The parameters $C_1\sim C_{12}$ in Eqs. (40), (41) and (43) are

$$\begin{aligned}C_1&=\frac{A_6F_3v_f\left(\frac{r_i}{r_f}\right)^{m_1-1}}{\left(\frac{r_i}{r_f}\right)^{m_2-1}F_1F_4-\left(\frac{r_i}{r_f}\right)^{m_1-1}F_2F_3}\frac{m_2-1}{1+m_1}\left[\left(\frac{r_i}{r_f}\right)^{-(m_1+1)}-1\right]\\
&\quad-\frac{A_5F_4v_f\left(\frac{r_i}{r_f}\right)^{m_2-1}}{\left(\frac{r_i}{r_f}\right)^{m_2-1}F_1F_4-\left(\frac{r_i}{r_f}\right)^{m_1-1}F_2F_3}\frac{m_1-1}{1+m_2}\left[\left(\frac{r_i}{r_f}\right)^{-(m_2+1)}-1\right]\end{aligned}\tag{A.9}$$

$$\begin{aligned}C_2&=\frac{A_5F_4S_1\left(\frac{r_i}{r_f}\right)^{m_2-1}-\frac{E_f}{E_m}A_5F_2S_2}{\left(\frac{r_i}{r_f}\right)^{m_2-1}F_1F_4-\left(\frac{r_i}{r_f}\right)^{m_1-1}F_2F_3}\frac{m_1-1}{1+m_2}\left[\left(\frac{r_i}{r_f}\right)^{-(m_2+1)}-1\right]\\
&\quad\times\frac{A_6F_3S_1\left(\frac{r_i}{r_f}\right)^{m_1-1}-\frac{E_f}{E_m}A_6F_1S_2}{\left(\frac{r_i}{r_f}\right)^{m_2-1}F_1F_4-\left(\frac{r_i}{r_f}\right)^{m_1-1}F_2F_3}\frac{m_2-1}{1+m_1}\left[\left(\frac{r_i}{r_f}\right)^{-(m_1+1)}-1\right]\end{aligned}\tag{A.10}$$

$$\begin{aligned}C_3&=\frac{E_f}{E_m}\left\{\frac{A_5F_2v_m}{\left(\frac{r_i}{r_f}\right)^{m_2-1}F_1F_4-\left(\frac{r_i}{r_f}\right)^{m_1-1}F_2F_3}\frac{m_1-1}{1+m_2}\right.\\
&\quad\left.\times\left[\left(\frac{r_i}{r_f}\right)^{-(m_2+1)}-1\right]-\frac{A_6F_1v_m}{\left(\frac{r_i}{r_f}\right)^{m_2-1}F_1F_4-\left(\frac{r_i}{r_f}\right)^{m_1-1}F_2F_3}\frac{m_2-1}{1+m_1}\left[\left(\frac{r_i}{r_f}\right)^{-(m_1+1)}-1\right]\right\}\end{aligned}\tag{A.11}$$

$$\begin{aligned}C_4&=\frac{\overline{A}_5\overline{F}_4E_f(v_i-v_f)\left(\frac{r_i}{r_f}\right)^{\bar{m}_2-1}-\overline{A}_5\overline{F}_2E_f(v_i-v_m)}{\left(\frac{r_i}{r_f}\right)^{\bar{m}_2-1}\overline{F}_1\overline{F}_4-\left(\frac{r_i}{r_f}\right)^{\bar{m}_1-1}\overline{F}_2\overline{F}_3}\\
&\quad\times\frac{\bar{m}_1-1}{1+\bar{m}_2}\left[\left(\frac{r_i}{r_f}\right)^{-(\bar{m}_2+1)}-1\right]\\
&\quad-\frac{\overline{A}_6\overline{F}_3E_f(v_i-v_f)\left(\frac{r_i}{r_f}\right)^{\bar{m}_1-1}-\overline{A}_6\overline{F}_1E_f(v_i-v_m)}{\left(\frac{r_i}{r_f}\right)^{\bar{m}_2-1}\overline{F}_1\overline{F}_4-\left(\frac{r_i}{r_f}\right)^{\bar{m}_1-1}\overline{F}_2\overline{F}_{3_3}}\\
&\quad\times\frac{\bar{m}_2-1}{1+\bar{m}_1}\left[\left(\frac{r_i}{r_f}\right)^{-(\bar{m}_1+1)}-1\right]\end{aligned}\tag{A.12}$$

$$\begin{aligned}C_5&=\frac{\overline{A}_5\overline{F}_4E_f\left(\frac{r_i}{r_f}\right)^{\bar{m}_2-1}}{\left(\frac{r_i}{r_f}\right)^{\bar{m}_2-1}\overline{F}_1\overline{F}_4-\left(\frac{r_i}{r_f}\right)^{\bar{m}_1-1}\overline{F}_2\overline{F}_3}\frac{\bar{m}_1-1}{1+\bar{m}_2}\left[\left(\frac{r_i}{r_f}\right)^{-(\bar{m}_2+1)}-1\right]\\
&\quad-\frac{\overline{A}_6\overline{F}_3E_f\left(\frac{r_i}{r_f}\right)^{\bar{m}_1-1}}{\left(\frac{r_i}{r_f}\right)^{\bar{m}_2-1}\overline{F}_1\overline{F}_4-\left(\frac{r_i}{r_f}\right)^{\bar{m}_1-1}\overline{F}_2\overline{F}_3}\frac{\bar{m}_2-1}{1+\bar{m}_1}\left[\left(\frac{r_i}{r_f}\right)^{-(\bar{m}_1+1)}-1\right]\end{aligned}\tag{A.13}$$

$$
\begin{aligned}
C_6 = {} & \frac{\bar{A}_6 \bar{F}_1 E_f}{\left(\frac{r_i}{r_f}\right)^{\bar{m}_2-1} \bar{F}_1 \bar{F}_4 - \left(\frac{r_i}{r_f}\right)^{\bar{m}_1-1} \bar{F}_2 \bar{F}_3} \\
& \times \frac{\bar{m}_2 - 1}{1 + \bar{m}_1} \left[\left(\frac{r_i}{r_f}\right)^{-(\bar{m}_1+1)} - 1 \right] \\
& - \frac{\bar{A}_5 \bar{F}_2 E_f}{\left(\frac{r_i}{r_f}\right)^{\bar{m}_2-1} \bar{F}_1 \bar{F}_4 - \left(\frac{r_i}{r_f}\right)^{\bar{m}_1-1} \bar{F}_2 \bar{F}_3} \\
& \times \frac{\bar{m}_1 - 1}{1 + \bar{m}_2} \left[\left(\frac{r_i}{r_f}\right)^{-(\bar{m}_2+1)} - 1 \right]
\end{aligned} \tag{A.14}
$$

$$
\begin{aligned}
C_7 = {} & \frac{B_2}{2(1+\nu_m)B_3} \left[\frac{2\nu_m r_i^2 H_5}{(r_m^2 - r_i^2) H_8} + \frac{E_m \nu_i}{E_i} \frac{H_{12}}{H_8} \right] \\
& + \frac{\nu_i C_1}{2(1+\nu_i) I_i}
\end{aligned} \tag{A.15}
$$

$$
\begin{aligned}
C_8 = {} & \frac{B_2}{2(1+\nu_m)B_3} \left[\frac{2\nu_m r_i^2 H_6}{(r_m^2 - r_i^2) H_8} - \frac{E_m}{E_i} + \frac{E_m \nu_i H_{13}}{E_i H_8} \right] \\
& + \frac{\nu_i C_2}{2(1+\nu_i) I_i} - \left(1 - \frac{2\nu_i^2}{1-\nu_i}\right) \frac{Q \ln(r_i/r_f)}{2(1+\nu_i)}
\end{aligned} \tag{A.16}
$$

$$
\begin{aligned}
C_9 = {} & \frac{B_2}{2(1+\nu_m)B_3} \left[1 + \frac{2\nu_m r_i^2 H_7}{(r_m^2 - r_i^2) H_8} + \frac{E_m \nu_i}{E_i} \frac{H_{14}}{H_8} \right] \\
& + \frac{\nu_i C_3}{2(1+\nu_i) I_i}
\end{aligned} \tag{A.17}
$$

$$
\begin{aligned}
C_{10} &= \frac{2\nu_m r_i^2 H_5}{(r_m^2 - r_i^2) H_8} + \frac{E_m \nu_i H_{12}}{E_i H_8}, \\
C_{11} &= \frac{2\nu_m r_i^2 H_6}{(r_m^2 - r_i^2) H_8} - \frac{E_m}{E_i} + \frac{E_m \nu_i H_{13}}{E_i H_8}, \\
C_{12} &= 1 + \frac{2\nu_m r_i^2 H_7}{(r_m^2 - r_i^2) H_8} + \frac{E_m \nu_i H_{14}}{E_i H_8}
\end{aligned} \tag{A.18}
$$

Appendix B

In the case with the Young's modulus of interphase varying according to a linear graded law, the coefficients $F_1 \sim F_4$, S_1, S_2 in Eq. (63) are

$$
\begin{aligned}
F_1 &= \left[\frac{y_1(r)}{r} - \frac{1-\nu_f}{I_i} A_1(r) \right]_{r=r_f}, \quad F_2 = \left[\frac{y_2(r)}{r} - \frac{1-\nu_f}{I_i} A_2(r) \right]_{r=r_f} \\
F_3 &= \left[\frac{y_1(r)}{r} + \frac{(1+\nu_m^2) r_m^2 + (1-\nu_m) r_i^2}{I_i (r_m^2 - r_i^2)} A_1(r) \right]_{r=r_i} \\
F_4 &= \left[\frac{y_2(r)}{r} + \frac{(1+\nu_m^2) r_m^2 + (1-\nu_m) r_i^2}{I_i (r_m^2 - r_i^2)} A_2(r) \right]_{r=r_i} \\
S_1 &= \frac{\nu_i}{1-\nu_i}(1-\nu_f), \quad S_2 = -\frac{\nu_i}{1-\nu_i} \frac{(1+\nu_m^2) r_m^2 + (1-\nu_m) r_i^2}{r_m^2 - r_i^2}
\end{aligned} \tag{B.1}
$$

Then, $H_1 \sim H_7$ in Eq. (63) can be expressed as

$$
\begin{aligned}
H_1 &= \frac{\nu_f}{I_i} [A_2(r_f) F_3 - A_1(r_f) F_4] \\
H_2 &= \frac{1}{I_i} [A_1(r_f) F_4 S_1 - \frac{E_f}{E_m} A_1(r_f) F_2 S_2 + \frac{E_f}{E_m} A_2(r_f) F_1 S_2 \\
&\quad - A_2(r_f) F_3 S_1] + \frac{H_4 \nu_i}{1-\nu_i} \\
H_3 &= \frac{E_f \nu_m}{E_m I_i} [A_1(r_f) F_2 - A_2(r_f) F_1], \quad H_4 = F_1 F_4 - F_2 F_3 \\
H_5 &= \frac{E_m \nu_f}{E_f I_i} [A_2(r_i) F_3 - A_1(r_i) F_4] \\
H_6 &= \frac{E_m}{E_f I_i} \Big[A_1(r_i) F_4 S_1 - \frac{E_f}{E_m} A_1(r_i) F_2 S_2 \\
&\quad + \frac{E_f}{E_m} A_2(r_i) F_1 S_2 - A_2(r_i) F_3 S_1 \Big] + \frac{H_4 \nu_i}{1-\nu_i} \\
H_7 &= \frac{\nu_m}{I_i} [A_1(r_i) F_2 - A_2(r_i) F_1]
\end{aligned} \tag{B.2}
$$

and $H_8 \sim H_{13}$ in Eq. (64) are

$$
\begin{aligned}
H_8 &= \frac{\nu_f}{I_i} [A_6(r_f) F_3 - A_5(r_f) F_4] \\
H_9 &= \frac{1}{I_i} \left[A_5(r_f) F_4 S_1 - \frac{E_f}{E_m} A_5(r_f) F_2 S_2 + \frac{E_f}{E_m} A_6(r_f) F_1 S_2 - A_6(r_f) F_3 S_1 \right] + \frac{2H_4 \nu_i}{1-\nu_i} \\
H_{10} &= \frac{E_f \nu_m}{E_m I_i} [A_5(r_f) F_2 - A_6(r_f) F_1], \quad H_{11} = \frac{E_m \nu_f}{E_f I_i} [A_6(r_i) F_3 - A_5(r_i) F_4] \\
H_{12} &= \frac{E_m}{E_f I_i} \left[A_5(r_i) F_4 S_1 - \frac{E_f}{E_m} A_5(r_i) F_2 S_2 + \frac{E_f}{E_m} A_6(r_i) F_1 S_2 - A_6(r_i) F_3 S_1 \right] + \frac{2H_4 \nu_i}{1-\nu_i} \\
H_{13} &= \frac{\nu_m}{I_i} [A_5(r_i) F_2 - A_6(r_i) F_1]
\end{aligned} \tag{B.3}
$$

The functions $A_1(r)$, $A_2(r)$, $A_5(r)$, $A_6(r)$ in Eqs. (B.1), (B.2), (B.3) can be found in Eq. (62).

In the part of thermal residual stress, the coefficients $\bar{F}_1 \sim \bar{F}_4$ in Eq. (68) are

$$
\begin{aligned}
\bar{F}_1 &= \left[\frac{\bar{y}_1(r)}{r} - \frac{I_f}{I_i(1+\nu_f)} \bar{A}_1(r) \right]_{r=r_f}, \quad \bar{F}_2 = \left[\frac{\bar{y}_2(r)}{r} - \frac{I_f}{I_i(1+\nu_f)} \bar{A}_2(r) \right]_{r=r_f} \\
\bar{F}_3 &= \left\{ \frac{\bar{y}_1(r)}{r} + \frac{I_m}{I_i(1+\nu_m)} \left[\frac{r_i^2}{(r_m^2 - r_i^2)} + \frac{r_m^2}{(1-2\nu_m)(r_m^2 - r_i^2)} \right] \bar{A}_1(r) \right\}_{r=r_i} \\
\bar{F}_4 &= \left\{ \frac{\bar{y}_2(r)}{r} + \frac{I_m}{I_i(1+\nu_m)} \left[\frac{r_i^2}{(r_m^2 - r_i^2)} + \frac{r_m^2}{(1-2\nu_m)(r_m^2 - r_i^2)} \right] \bar{A}_2(r) \right\}_{r=r_i}
\end{aligned} \tag{B.4}
$$

Then, the coefficients $K_1 \sim K_9$ in Eq. (68) can be expressed as

$$
K_1 = I_f \frac{[\bar{A}_1(r_f)\bar{F}_4 - \bar{A}_2(r_f)\bar{F}_3](\nu_i - \nu_f) + [\bar{A}_2(r_f)\bar{F}_1 - \bar{A}_1(r_f)\bar{F}_2](\nu_i - \nu_m)}{I_i(1+\nu_f)(\bar{F}_1\bar{F}_4 - \bar{F}_2\bar{F}_3)} - \nu_f
$$

$$
K_2 = \frac{I_f}{I_i(1+\nu_f)} \frac{\bar{A}_1(r_f)\bar{F}_4 - \bar{A}_2(r_f)\bar{F}_3}{\bar{F}_1\bar{F}_4 - \bar{F}_2\bar{F}_3},
$$

$$
K_3 = \frac{I_f}{I_i(1+\nu_f)} \frac{\bar{A}_2(r_f)\bar{F}_1 - \bar{A}_1(r_f)\bar{F}_2}{\bar{F}_1\bar{F}_4 - \bar{F}_2\bar{F}_3}
$$

$$
K_4 = -\frac{I_m r_i^2}{I_i} \frac{[\bar{A}_1(r_i)\bar{F}_4 - \bar{A}_2(r_i)\bar{F}_3](\nu_i - \nu_f) + [\bar{A}_2(r_i)\bar{F}_1 - \bar{A}_1(r_i)\bar{F}_2](\nu_i - \nu_m)}{(r_m^2 - r_i^2)(1+\nu_m)[\bar{F}_1\bar{F}_4 - \bar{F}_2\bar{F}_3]} - \nu_m
$$

$$
K_5 = -\frac{I_m r_i^2}{I_i} \frac{\bar{A}_1(r_i)\bar{F}_4 - \bar{A}_2(r_i)\bar{F}_3}{(r_m^2 - r_i^2)(1+\nu_m)[\bar{F}_1\bar{F}_4 - \bar{F}_2\bar{F}_3]}
$$

$$
K_6 = -\frac{I_m r_i^2}{I_i} \frac{\bar{A}_2(r_i)\bar{F}_1 - \bar{A}_1(r_i)\bar{F}_2}{(r_m^2 - r_i^2)(1+\nu_m)[\bar{F}_1\bar{F}_4 - \bar{F}_2\bar{F}_3]}
$$

$$K_7 = \frac{E_f r_f^2}{2I_f}\left[\left(1 - v_f^2\right) + 2v_f(1 + v_f)K_1\right] + \frac{(r_m^2 - r_i^2)E_m}{2I_m}\left[(1 - v_m^2) + 2v_m(1 + v_m)K_4\right] + M_1$$

$$K_8 = \frac{E_f v_f r_f^2}{I_f}(1 + v_f)K_2 + \frac{(r_m^2 - r_i^2)E_m}{I_m} v_m(1 + v_m)K_5 + M_2$$

$$K_9 = \frac{E_f v_f r_f^2}{I_f}(1 + v_f)K_3 + \frac{(r_m^2 - r_i^2)E_m}{I_m} v_m(1 + v_m)K_6 + M_3 \quad (B.5)$$

in which

$$M_1 = P_0 + \frac{v_i(1 + v_i)}{I_i}\frac{(P_1\bar{F}_4 - P_2\bar{F}_3)(v_i - v_f) + (P_2\bar{F}_1 - P_1\bar{F}_2)(v_i - v_m)}{\bar{F}_1\bar{F}_4 - \bar{F}_2\bar{F}_3}$$

$$M_2 = \frac{v_i(1 + v_i)}{I_i}\frac{P_1\bar{F}_4 - P_2\bar{F}_3}{\bar{F}_1\bar{F}_4 - \bar{F}_2\bar{F}_3}, \quad M_3 = \frac{v_i(1 + v_i)}{I_i}\frac{P_2\bar{F}_1 - P_1\bar{F}_2}{\bar{F}_1\bar{F}_4 - \bar{F}_2\bar{F}_3} \quad (B.6)$$

$$P_0 = \frac{a}{2}\left(r_i^2 - r_f^2\right) + \frac{b}{3}\left(r_i^3 - r_f^3\right)$$

$$P_1 = \int_{r_f}^{r_i} E_i[r\bar{y}_1'(r) + \bar{y}_1(r)]dr, \quad P_2 = \int_{r_f}^{r_i} E_i[r\bar{y}_2'(r) + \bar{y}_2(r)]dr$$

a, b satisfy Eq. (55). The coefficients $K_{10} \sim K_{15}$ in Eq. (69) are given as

$$K_{10} = \frac{E_f}{I_i}\frac{[\bar{A}_5(r_f)\bar{F}_4 - \bar{A}_6(r_f)\bar{F}_3](v_i - v_f) + [\bar{A}_6(r_f)\bar{F}_1 - \bar{A}_5(r_f)\bar{F}_2](v_i - v_m)}{\bar{F}_1\bar{F}_4 - \bar{F}_2\bar{F}_3}$$

$$K_{11} = \frac{E_f}{I_i}\frac{\bar{A}_5(r_f)\bar{F}_4 - \bar{A}_6(r_f)\bar{F}_3}{\bar{F}_1\bar{F}_4 - \bar{F}_2\bar{F}_3}, \quad K_{12} = \frac{E_f}{I_i}\frac{\bar{A}_6(r_f)\bar{F}_1 - \bar{A}_5(r_f)\bar{F}_2}{\bar{F}_1\bar{F}_4 - \bar{F}_2\bar{F}_3} \quad (B.7)$$

$$K_{13} = \frac{E_m}{I_i}\frac{[\bar{A}_5(r_i)\bar{F}_4 - \bar{A}_6(r_i)\bar{F}_3](v_i - v_f) + [\bar{A}_6(r_i)\bar{F}_1 - \bar{A}_5(r_i)\bar{F}_2](v_i - v_m)}{\bar{F}_1\bar{F}_4 - \bar{F}_2\bar{F}_3}$$

$$K_{14} = \frac{E_m}{I_i}\frac{\bar{A}_5(r_i)\bar{F}_4 - \bar{A}_6(r_i)\bar{F}_3}{\bar{F}_1\bar{F}_4 - \bar{F}_2\bar{F}_3}, \quad K_{15} = \frac{E_m}{I_i}\frac{\bar{A}_6(r_i)\bar{F}_1 - \bar{A}_5(r_i)\bar{F}_2}{\bar{F}_1\bar{F}_4 - \bar{F}_2\bar{F}_3}$$

In Eqs. (B.4), (B.5) and (B.7), the functions $\bar{A}_1(r), \bar{A}_2(r), \bar{A}_5(r), \bar{A}_6(r)$ can be found in Eq. (67).

The parameters $C_1 \sim C_6$ in Eq. (72) are expressed as

$$C_1 = \frac{v_f}{E_f}\frac{V_2F_3 - V_1F_4}{F_1F_4 - F_2F_3}, \quad C_2 = \frac{1}{E_f}\frac{(V_1F_4 - V_2F_3)S_1 + \frac{E_f}{E_m}S_2(V_2F_1 - V_1F_2)}{F_1F_4 - F_2F_3}$$

$$C_3 = \frac{v_m}{E_m}\frac{V_1F_2 - V_2F_1}{F_1F_4 - F_2F_3}, \quad C_4 = \frac{(\bar{V}_1\bar{F}_4 - \bar{V}_2\bar{F}_3)(v_i - v_f) + (\bar{V}_2\bar{F}_1 - \bar{V}_1\bar{F}_2)(v_i - v_m)}{\bar{F}_1\bar{F}_4 - \bar{F}_2\bar{F}_3}$$

$$C_5 = \frac{\bar{V}_1\bar{F}_4 - \bar{V}_2\bar{F}_3}{\bar{F}_1\bar{F}_4 - \bar{F}_2\bar{F}_3}, \quad C_6 = \frac{\bar{V}_2\bar{F}_1 - \bar{V}_1\bar{F}_2}{\bar{F}_1\bar{F}_4 - \bar{F}_2\bar{F}_3} \quad (B.8)$$

in which

$$V_1 = \int_{r_f}^{r_i} A_7(r)dr = \int_{r_f}^{r_i}\left[(a + br)\frac{dA_5(r)}{dr}\right]dr$$

$$V_2 = \int_{r_f}^{r_i} A_8(r)dr = \int_{r_f}^{r_i}\left[(a + br)\frac{dA_6(r)}{dr}\right]dr$$

$$\bar{V}_1 = \int_{r_f}^{r_i} \bar{A}_7(r)dr = \int_{r_f}^{r_i}\left[(a + br)\frac{d\bar{A}_5(r)}{dr}\right]dr \quad (B.9)$$

$$\bar{V}_2 = \int_{r_f}^{r_i} \bar{A}_8(r)dr = \int_{r_f}^{r_i}\left[(a + br)\frac{d\bar{A}_6(r)}{dr}\right]dr$$

The parameters $C_7 \sim C_{12}$ in Eq. (74) are given as follows,

$$C_7 = \frac{B_2}{2(1 + v_m)B_3}\left[\frac{2v_m r_i^2 H_5}{(r_m^2 - r_i^2)H_4} + \frac{E_m v_i H_{11}}{E_i H_4}\right] - \frac{v_i C_1}{2(1 + v_i)I_i}$$

$$C_8 = \frac{B_2}{2(1 + v_m)B_3}\left[\frac{2v_m r_i^2 H_6}{(r_m^2 - r_i^2)H_4} - \frac{E_m}{E_i} + \frac{E_m v_i}{E_i}\frac{H_{12}}{H_4}\right] - \frac{v_i C_2}{2(1 + v_i)I_i} - \frac{1}{2(1 + v_i)}\left(1 - \frac{2v_i^2}{1 - v_i}\right)\ln(E_m/E_f)$$

$$C_9 = \frac{B_2}{2(1 + v_m)B_3}\left[1 + \frac{2v_m r_i^2 H_7}{(r_m^2 - r_i^2)H_4} + \frac{E_m v_i H_{13}}{E_i H_4}\right] - \frac{v_i C_3}{2(1 + v_i)I_i}$$

$$C_{10} = \frac{2v_m r_i^2 H_5}{(r_m^2 - r_i^2)H_4} + \frac{E_m v_i H_{11}}{E_i H_4}, \quad C_{11} = \frac{2v_m r_i^2 H_6}{(r_m^2 - r_i^2)H_4} - \frac{E_m}{E_i} + \frac{E_m v_i}{E_i}\frac{H_{12}}{H_4}$$

$$C_{12} = 1 + \frac{2v_m r_i^2 H_7}{(r_m^2 - r_i^2)H_4} + \frac{E_m v_i H_{13}}{E_i H_4} \quad (B.10)$$

References

Afonso, J.C., Ranalli, G., 2005. Elastic properties of three-phase composites: analytical model based on the modified shear-lag model and the method of cells. Compos. Sci. Technol. 65 (7–8), 1264–1275.

Atkins, A.G., 1975. Intermittent bonding for high toughness/ high strength composites. J. Mater. Sci. 10 (5), 819–832.

Chai, Y.S., Mai, Y.W., 2001. New analysis on the fiber push-out problem with interface roughness and thermal residual stresses. J. Mater. Sci. 36 (8), 2095–2104.

Chen, S.H., Yan, C., Zhang, P., Gao, H.J., 2009. Mechanics of adhesive contact on a power-law graded elastic half-space. J. Mech. Phys. Solids 57 (9), 1437–1448.

Christensen, R.M., Lo, K.H., 1979. Solutions for effective shear properties in three phase sphere and cylinder models. J. Mech. Phys. Solids 27 (4), 315–330.

Cox, H.L., 1952. The elasticity and strength of paper and other fibrous materials. Br. J. Appl. Phys. 3 (3), 72–79.

Drzal, L.T., 1986. The interphase in epoxy composites. In: Dusek, K. (Ed.), Epoxy Resins and Composites II, Advances in Polymer Science, vol. 75. Springer-Verlag, Berlin, pp. 1–32.

Fu, S.Y., Yue, C.Y., Hu, X., Mai, Y.W., 2000a. Analyses of the micromechanics of stress transfer in single-and multi-fiber pull-out tests. Compos. Sci. Technol. 60 (4), 569–579.

Fu, S.Y., Yue, C.Y., Hu, X., Mai, Y.W., 2000b. On the elastic stress transfer and longitudinal modulus of unidirectional multi-short-fiber composites. Compos. Sci. Technol. 60 (16), 3001–3012.

Fu, S.Y., Feng, X.Q., Lauke, B., Mai, Y.W., 2008. Effects of particle size, particle/matrix interface adhesion and particle loading on mechanical properties of particulate-polymer composites. Compos. Part B 39 (6), 933–961.

Gao, X.L., Li, K., 2005. A shear-lag model for carbon nanotube-reinforced polymer composites. Int. J. Solids Struct. 42 (5–6), 1649–1667.

Gao, S.L., Mader, E., 2002. Characterisation of interphase nanoscale property variations in glass fibre reinforced polypropylene and epoxy resin composites. Compos. Part A 33 (4), 559–576.

Gao, Y.C., Mai, Y.W., Cotterell, B., 1988. Fracture of fiber-reinforced materials. J. Appl. Math. Phys. (ZAMP) 39 (4), 550–572.

Giannakopoulos, A.E., Pallot, P., 2000. Two-dimensional contact analysis of elastic graded materials. J. Mech. Phys. Solids 48 (8), 1597–1631.

Hashin, Z., 1990. Thermoelastic properties of fiber composites with imperfect interface. Mech. Mater. 8 (4), 333–348.

Hayes, S.A., Lane, R., Jones, F.R., 2001. Fibre/matrix stress transfer through a discrete interphase. Part 1—single-fiber model composites. Compos. Part A 32 (3–4), 379–389.

Huang, W., Rokhlin, S.I., 1996. Generalized self-consistent model for composites with functionally graded and multilayered interphases. Transfer matrix approach. Mech. Mater. 22 (3), 219–247.

Huang, Y.L., Young, R.J., 1996. Interfacial micromechanics in thermoplastic and thermosetting matrix carbon fiber composites. Compos. Part A 27 (10), 973–980.

Hughes, J.D.H., 1991. The carbon fiber/epoxy interface—A review. Compos. Sci. Technol. 41 (1), 31–45.

Jayaraman, K., Reifsnider, K.L., 1992. Residual stresses in a composite with continuously varying Young's modulus in the fiber/matrix interphase. J. Compos. Mater. 26 (6), 770–791.

Jayaraman, K., Reifsnider, K.L., 1993. The interphase in unidirectional fiber-reinforced epoxies: effect on residual thermal stresses. Compos. Sci. Technol. 47 (2), 119–129.

Jiang, Y.P., Gao, W.L., Yang, H., 2008. Numerical studies on the effective shear modulus of particle reinforced composites with an inhomogeneous inter-phase. Comput. Mater. Sci. 43 (4), 724–731.

Johnson, D.E., Johnson, J.R., 1965. Mathematical Methods in Engineering and Physics. Ronald, New York, pp. 42–50.
Kiritsi, C.C., Anifantis, N.K., 2001. Load carrying characteristics of short fiber composites containing a heterogeneous interphase region. Comput. Mater. Sci. 20 (1), 86–97.
Lauke, B., 2006. Determination of adhesion strength between a coated particle and polymer matrix. Compos. Sci. Technol. 66 (16), 3153–3160.
Leveque, D., Auvray, M.H., 1996. Study of carbon-fiber strain in model composites by Raman spectroscopy. Compos. Sci. Technol. 56 (7), 749–754.
Liu, H.Y., Zhou, L.M., Mai, Y.W., 1994. On fiber pull-out with a rough interface. Philos. Mag. A 70 (2), 359–372.
Liu, L., Song, Y.J., Fu, H.J., Jiang, Z.X., Zhang, X.Z., Wu, L.N., Huang, Y.D., 2008. The effect of interphase modification on carbon fiber/ polyarylacetylene resin composites. Appl. Surf. Sci. 254 (17), 5342–5347.
Low, B.Y., Gardner, S.D., Pittman, Jr. C.U., Hackett, R.M., 1995. A micromechanical characterization of residual thermal stresses in carbon fiber/epoxy composites containing a non-uniform interphase region. Compos. Eng. 5 (4), 375–396.
Lutz, M.P., Zimmerman, R.W., 2005. Effect of an inhomogeneous interphase zone on the bulk modulus and conductivity of a particulate composite. Int. J. Solids Struct. 42 (2), 429–437.
Mogilevskaya, S.G., Crouch, S.L., 2004. A Galerkin boundary integral method for multiple circular elastic inclusions with uniform interphase layers. Int. J. Solids Struct. 41 (5–6), 1285–1311.
Monette, L., Anderson, M.P., Grest, G.S., 1993. Effect of interphase modulus and cohesive energy on the critical aspect ratio in short-fibre composites. J. Mater. Sci. 28 (1), 79–99.
Naslain, R.R., 1998. The design of the fibre-matrix interfacial zone in ceramic matrix composites. Compos. Part A 29 (9-10), 1145–1155.
Needleman, A., Borders, T.L., Brinson, L.C., Flores, V.M., Schadler, L.S., 2010. Effect of an interphase region on debonding of a CNT reinforced polymer composite. Compos. Sci. Technol. 70 (15), 2207–2215.
Qiu, Y.P., Weng, G.J., 1991. Elastic moduli of thickly coated particle and fiber-reinforced composites. ASME J. Appl. Mech. 58 (2), 388–398.
Rjafiallah, S., Guessasma, S., Bizot, H., 2010. Effect of surface etching on interphase and elastic properties of a biocomposite reinforced using glass–silica particles. Compos. Sci. Technol. 70 (8), 1272–1279.
Romanowicz, M., 2010. Progressive failure analysis of unidirectional fiber-reinforced polymers with inhomogeneous interphase and randomly distributed fibers under transverse tensile loading. Compos. Part A 41 (12), 1829–1838.
Shen, L.X., Li, J., 2003. Effective elastic moduli of composites reinforced by particle or fiber with an inhomogeneous interphase. Int. J. Solids Struct. 40 (6), 1393–1409.
DS SIMULIA, 2010. Abaqus user's manual, Ver. 6.10.
Song, D.Y., Takeda, N., Shioya, T., Nakata, K., 1996. Approximate analysis of the stress state near the fiber ends of short fiber-reinforced composites and the consequent micro-fracture mechanisms. Compos. Part A 27 (5), 357–364.
Suresh, S., Giannakopoulos, A.E., Alcala, J., 1997. Spherical indentation of compositionally graded materials: theory and experiments. Acta Mater. 45 (4), 1307–1321.
Swain, R.E., Reifsnider, K.L., Jayaraman, K., El-Zein, M., 1990. Interface/ interphase concepts in composite material systems. J. Thermoplast. Compos. Mater. 3 (1), 13–23.
Theocaris, P.S., 1990. Diffusion-based adhesive bonds between phases in fibrous composites. Colloid Polym. Sci. 268 (5), 414–425.
Tsai, H.C., Arocho, A.M., Gause, L.W., 1990. Prediction of fiber-matrix interphase properties and their influence on interface stress, displacement and fracture toughness of composite material. Mater. Sci. Eng. A 126 (1-2), 295–304.
Wang, J.L., Crouch, S.L., Mogilevskaya, S.G., 2006. Numerical modeling of the elastic behavior of fiber-reinforced composites with inhomogeneous interphases. Compos. Sci. Technol. 66 (1), 1–18.
Whitney, J.M., Riley, M.B., 1966. Elastic properties of fiber reinforced composite materials. AIAA. J. 4 (9), 1537–1542.
Williams, J.G., James, M.R., Morris, W.L., 1994. Formation of the interphase in organic-matrix composites. Composites 25 (7), 757–762.
Wu, W., Verpoest, I., Varna, J., 1997. An improved analysis of the stresses in a single-fibre fragmentation test—II. 3-phase model. Compos. Sci. Technol. 58 (1), 41–50.
Yang, F., Pitchumani, R., 2004. Effects of interphase formation on the modulus and stress concentration factor of fiber-reinforced thermosetting-matrix composites. Compos. Sci. Technol. 64 (10–11), 1437–1452.
Zhang, J., He, C., 2008. A three-phase cylindrical shear-lag model for carbon nanotube composites. Acta Mech. 196 (1–2), 33–54.
Zhang, B.M., Yang, Z., Sun, X.Y., 2010. Measurement and analysis of residual stresses in single fiber composite. Mater. Des. 31 (3), 1237–1241.